Eidgenössische Technische Hochschule Zürich
Swiss Federal Institute of Technology Zurich

Master's Thesis

D-MTEC / D-BAUG

Fusion Methods for an MFD Estimation

Author:
Lukas Ambühl

Lead and Supervision:
Dr. Monica Menendez (IVT)
Prof. Dr. Paul Schönsleben (BWI)

6. Nov. 2015

Acknowledgements

First of all, I would like to thank Prof. Dr. Paul Schönsleben, who gave me the opportunity to follow an interesting field of current research within the scope of this master thesis. I would like to express my special gratitude to Dr. Monica Menendez, who supervised my work, for the great support, the helpful remarks and the interesting discussions. Furthermore, my thanks go to Javier Ortigosa, Jin Cao and Marco Rothenfluh, all from the institute for transport planning and Systems at ETH Zurich, for the pleasant and good exchange.

Abstract

In recent literature, the description and understanding of traffic conditions in urban networks on an aggregated level has been popularized. A promising framework is the macro fundamental diagram (MFD), relating average flow and average density in a more or less homogeneous urban network. The application of the MFD in traffic management and control are manifold. It has been shown that it can be used for an efficient perimeter control at city entries or for an evaluation of traffic policies at an aggregated level. However, its implementation requires an accurate estimation with the data sources available.

Especially loop detectors data (LDD) and floating car data (FCD), were examined *separately* in respect to their accuracy estimating the MFD. One important factor is the network coverage of the source considered. Only certain streets have loop detectors installed and only certain vehicles (or drivers) are equipped with devices sending information about their whereabouts. Having less data of that one source decreases the accuracy of the MFD.

This master's thesis proposes to estimate the MFD based on both data sources *simultaneously*. Thereby successful fusion methods were developed, where the LDD and the FCD are fused in respect to their accuracy and their network coverage. The most promising fusion always reduces the estimation error significantly, also if the network coverage of the FCD needs to be estimated with LDD. It separates the urban network into two sub-network, one with loop detectors and one without. The information from the LDD and the FCD is then weighted according to the sub-networks and the square root of the network coverage of the FCD.

Keywords MFD estimation; Simulation; Loop detectors; Floating Car Data (FCD); Fusion; Probe penetration estimation

Contents

1 Introduction **3**

2 Literature Review **5**
2.1 Early Macroscopic Models 5
2.2 Macroscopic Fundamental Diagram 5
2.3 Recent Developments in MFD Estimation 7

3 Methodology **11**
3.1 Traffic Simulation 11
3.2 Building the MFD 13
3.3 Estimation of Probe Penetration Rate 15
3.3.1 Probe Penetration Rate Known a-priori 15
3.3.2 Probe Penetration Rate not Known a-priori 16
3.4 Accuracy of an Estimated MFD 17
3.5 Fusion Methods 18
3.5.1 Method 0 19
3.5.2 Method 1 20
3.5.3 Method 2 20
3.5.4 Method 3 21
3.5.5 Method 4 22
3.5.6 Method 5 22

4 Results **23**
4.1 Probe Penetration Rate 23
4.2 Real MFD 23
4.3 Fusion Results 24
4.3.1 Method 0 25
4.3.2 Method 1 26
4.3.3 Method 2 28
4.3.4 Method 3 30
4.3.5 Method 4 31
4.3.6 Method 5 33

5 Analysis of Results **35**
5.1 Reference Method 36
5.2 Comparison of Methods 1-5 36
5.2.1 Cross-Comparison 36
5.2.2 Method 3 and Reference Method 38
5.3 Robustness of Methods 3 and 5 40
5.3.1 Measurement Errors 40
5.3.2 Loop Density Errors 41

6 Conclusions **43**
6.1 Main Findings 43
6.2 Future Research 44

Bibliography **47**

A Annex **49**

1 Introduction

In a study commissioned by the Swiss Federal Office for Spatial Development (ARE), it was found that 91% of the congested vehicle-hours in the Canton of Zurich are counted in urban areas (Keller and Wuethrich, 2012). Another publication by the Swiss Federal Road Office (ASTRA) showed that 85% of congestion is "recurring" (ASTRA, 2014), meaning due to capacity issues. Moreover, a recent study investigated the cost of congestion to be around 80 - 140 million Swiss Francs - only for the Canton of Zurich (Ernst Basler+Partner, 2008).

In other words, the overwhelming majority of congestion takes place in urban areas, is caused by capacity issues, and is responsible for yearly costs of up to 100 Swiss Francs to each inhabitant of the Canton of Zurich. Without having touched upon the topic of congestion externalities, such as noise, green house gas emissions, etc., it is obvious that strategies relieving urban networks from congestion are in need.

Infrastructure projects are expensive and in urban areas space is scarce - especially in European cities. Therefore, strategies were developed that do not involve big infrastructure projects, such as parking strategies, mobility pricing, perimeter control, etc. (Ernst Basler+Partner, 2008). However, in order to develop strategies that limit congestion *network-wide*, meaningful macroscopic parameters of networks must be found first. A promising framework developed by Daganzo (2007) is the **M**acro **F**undamental **D**iagram (MFD). The MFD relates average flow (e.g. how many vehicles per hour) and density (e.g. how many vehicles per km) of an urban network. Different sensors can be used to estimate the aforementioned parameters. Most widely used is data from loop detectors as well as floating car data. Loop detectors are static sensors, which evaluate the traffic condition, whereas floating car data is collected from vehicles driving in the network (Leclercq et al., 2014). Both are collected in real-time.

In reality, not all links in a network have loop detectors installed, nor are all vehicles (or drivers) equipped with devices that regularly send positioning data. Rather, there is a certain network coverage, e.g 10% of the links have a loop detector installed, and 15% of the vehicles have a GPS installed. Not surprisingly, the accuracy of an MFD estimated with a low network coverage is lower than one with a higher network coverage. However, since both types of data sources usually co-exist, it is of interest, if combining the results from each source can improve the overall estimation of the MFD.

It is the aim of this thesis to investigate if data acquired from different sources in a simulated network with incomplete coverage can ameliorate the estimation of an MFD by using simple fusion methods. Thereby, this thesis is structured as follows: Section 2 gives an overview of the literature regarding the MFD with an emphasis on recent findings on the estimation of the MFD with loop detectors or floating car data. In section 3, the simulation setup is explained and fusion methods are proposed. Results of the fusion methods are presented in section 4. In section 5, an analysis and comparison of the aforementioned results are presented. Finally, section 6 gives a conclusion and fields of further analysis are given.

2 Literature Review

This section gives an overview of the state-of-the-art regarding an estimation of the MFD with only limited amount of data: Methodologies on how loop detectors or floating car data can be used to estimate an MFD, in most cases, for a simulated network are presented. And, different definitions regarding the accuracy of an estimated MFD are introduced, based on either relative errors or on ratios incorporating the critical density.

2.1 Early Macroscopic Models

Different approaches were proposed in the past to model and understand urban traffic on an aggregated level. Ranging from models about the number of vehicles entering central area of a city (Smeed, 1968), to the modeling of central London using a linear speed-flow model (Thomson, 1967). However, a drawback to these concepts, was that they were only considering free flow conditions of traffic or slight congestion. It is then Godfrey (1969) who mentions the idea of the existence of a macroscopic relationship between the mean speed and the accumulation of vehicles in a network. The idea was later refined with the introduction of the idea to model traffic by two fluids, one representing the stopped vehicles - due to traffic light, congestion, etc. - while the other represented the moving vehicles (Herman and Prigogine, 1979). With this, the foundations for the existence of a macro fundamental diagram were laid.

2.2 Macroscopic Fundamental Diagram

Originally Geroliminis and Daganzo (2007) related the number of vehicles in a network (accumulation) and the number of vehicles reaching their destination (output or production) in the so-called macro fundamental diagram (MFD). This relationship can be translated into the more commonly used diagram where the average flows and average densities are represented on a macro level - on a network level. It can be seen as an analogy to the fundamental diagram (FD) which was originally proposed by Greenshields et al. (1935). The fundamental diagram gives the relation between the vehicle density and the vehicle flow of one link. A distinct curve (usually approximated in triangular shape) describes the link with a maximum flow at a critical density. Similarly, this relation can be observed for homogeneous urban networks: More and more vehicles can enter a network until it reaches its maximum capacity, any additional vehicles from this point on will then start inducing congestion. Note that, analogue to the FD, the slope in the MFD represents the average speed of the vehicles in the system (cf. fig. 1). Therefore, looking at speed, the network will exhibit the same speed until it reaches its maximum capacity (which corresponds to the flow at critical density); from then on, additional vehicles will start decreasing the mean speed in the network. (Daganzo, 2007)

In 2007 computer simulations of downtown San Francisco indicating the existence MFD were successfully conducted (Geroliminis and Daganzo, 2007). Afterwards, Geroliminis and Daganzo (2008) proved the existence of the MFD with real data, by using GPS data of taxis in a 10 km^2 network within the city of Yokohama, Japan. Thereby the following definition is given for weighted

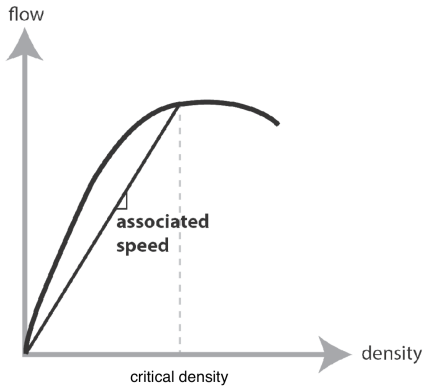

Figure 1: Typical MFD; (Gayah and Dixit, 2013).

averages: $q^w = \sum_i q_i l_i / \sum_i l_i$ and $k^w = \sum_i k_i l_i / \sum_i l_i$. q_i and k_i denote the flow and density on link i with length l_i.

Geroliminis and Daganzo (2007) showed that the MFD is a suitable instrument for a perimeter control strategy. Thereby, the network should always operate at or below the critical density (cf. fig. 1), in order to fully utilize the maximum capacity of the system. A perimeter is set up around the network preventing new vehicles to enter the system (e.g. longer red phases).

The analytic framework for MFDs was introduced using variational theory: Daganzo and Geroliminis (2008) proposed certain sufficient conditions for the existence of a theoretical MFD in a specific network, the so called regularity conditions: a distributed and slow-varying demand, a network where multiple route choices are possible including most links, and a network which is more or less homogeneous. Furthermore, the authors point out that obtaining a "well defined" MFD, meaning an MFD which shows low scatter, depends on the type of network and on the type of urban area. Freeway networks and polycentric urban areas are expected to display higher scatter than homogeneous, small networks. In other words, an MFD measured with real data for a certain network, may fall far from the well defined MFD that could be calculated analytically using variational theory for the identical network. The analytic MFD is therefore an upper bound for an MFD measured in reality.
Summarized, the MFD should be dependent solely on the network and not on the demand: A well-defined MFD has a maximum invariant to changes in time, demand or origin-destination table across days and congestion spreads more or less homogeneously (Mazloumian et al., 2010).

Later, Buisson and Ladier (2009) constructed MFDs using real data from 3 different days of the city of Toulouse, France, with the purpose of further investigating the aforementioned notion of homogeneity stated by Daganzo and Geroliminis (2008). The authors divided the sample in order to take the network properties into account. The data recovered by loop detectors was clustered according to the distance of the loop to the intersection, according to the road type (highway or urban road) and according to the roads location (peripheral

or center). The analysis showed that the distance between the loop detector and the traffic light has a strong impact on the shape of the MFD. If the loop detector is placed close to a traffic light, the periodic queue in front of the traffic light leads to an overestimation of the density in the network.
This is an important result which is confirmed by Courbon and Leclercq (2011): Densities measured by loop detectors should only be used with caution, their spatial dependency is a shortfall. However, if loop detectors are well distributed within the links of the network, then the *average* density estimate needed for an MFD is representative. Loop detectors on all links together need to be distributed in a way that they cover different traffic states (up-stream, down-stream, etc.). In other words, in one link the loop detector is placed close to the intersection, in another link it is placed further upstream, etc.

Buisson and Ladier (2009) confirmed that the homogeneity of the zone, the loading and unloading of congestion and how the data was collected were of importance for a low scatter MFD. Therefore, it is concluded that splitting the data into different sets of data according to the geographic location and its type of road is a prerequisite for obtaining a well defined MFD.
Geroliminis and Sun (2011) further investigated the properties of a well defined MFD by again using data from Yokohama. As a result the authors conclude that if two traffic states from two different time intervals have the same spatial distribution of link density, then the two time intervals have the same average flow. Thereby, the aforementioned assumption that congestion is evenly distributed across the network made by Daganzo and Geroliminis (2008)) is relaxed.

2.3 Recent Developments in MFD Estimation

Recently, MFD estimation methods were developed that incorporate the use of mobile probe data (a form of floating car data). Mobile probe data originates directly from vehicles traveling in the network itself. The type of data recovered depends on the device installed in the vehicle. Usually they include the current location, speed and acceleration. (Gayah and Dixit, 2013)

Gayah and Dixit (2013) explored the possibilities of using mobile probe data within a micro simulation of downtown Orlando. The authors of the study randomly assigned a fraction of vehicles in the network to serve as mobile probes. The so called mobile probe penetration rate ranged between 0.025 up to 0.5. In other words having a penetration rate of e.g., 0.3, means that 30% of the vehicles in the network supply information to the traffic controller. It is expected that the higher the penetration rate and the longer the observation period, the higher the accuracy of the information will be. That is to say, for a penetration rate of 0.3 we expect to see a higher accuracy than with 0.1. Moreover, observing the network for 300 s is expected to be more accurate than 100 s of observation. Using the average speed of the mobile probes, the average flow and density were estimated based on a known MFD (cf. fig. 1). A drawback mentioned in the paper is that when taking the average speed in order to estimate density and flow in an MFD, the accuracy is smaller in free-flow conditions. Gayah and Dixit (2013) used $\hat{k}/k$ as a proxy for the accuracy, where $\hat{k}$ stands for the estimated density and k stands for the real density (calculated with full network coverage;

in this case simulated). The results confirm the expectation about the probe penetration rate and the observation duration, stated above. However, even in the unlikely case where the penetration rate is 0.5, the estimates for the density varied between 0.8 and 1.3 of the real density for an observation period of 300 s. For lower, more realistic penetration rates, the proposed method did not prove to be sufficiently reliable. However an alternative method is proposed: Instead of estimating density and flow, the estimated values of the density were used to evaluate if the system was congested or not. This methodology has the advantage of comparing only two values - the estimated density and the critical density (indicated by the maximum flow). Whenever the estimated density was higher than the critical density, the state was assessed to be congested. If the system was then congested in reality, the prediction would be labeled as "correct", otherwise "missed". Taking this methodology, the authors of the study were able to accurately identify the traffic states (congested/uncongested) with a mobile probe penetration rate as small as 7.5% and an observation period of 300s. The reliance on an MFD known a-priori is a limitation to this study.

Ortigosa et al. (2014) studied the influence of the location and number of measurement points for an MFD perimeter control. Unlike discussed by Buisson and Ladier (2009) the placement of the loop detector within the link was not in question. In fact, Ortigosa et al. (2014) placed loop detectors optimally within a link - queues upstream of a traffic light do not distort the density measurements. They employed a VISSIM micro simulation of downtown Zurich, created an MFD with only a subset of all the links (partial MFD) and calculated the accuracy thereof compared to a real MFD (measured with all links). Different strategies were defined for choosing the subset of links (random, distance to the center, street hierarchy and existence of traffic light downstream) and tested at different levels of coverage (e.g. 5% of the links used in the subset). Furthermore a quasi-optimal selection strategy was introduced. The accuracy of a partial MFD is defined differently than previous scholars have proposed: The authors introduce a density ratio between the density and the critical density for each time slice. According to Ortigosa et al. (2014), an MFD is 100% accurate if the density ratios of the partial MFD are exactly the same as in the complete MFD for every time step. Furthermore, the paper investigates a system employed by the city of Zurich, ZuriTraffic. It is concluded that the level of coverage is the decisive parameter for the accuracy and not so much the strategy used to create the partial MFD. A link coverage of 25% ensures an error of less than 15 percentage points between the density ratio of the partial MFD and the real MFD. The authors mention that the limitations of their study can be found in the nontransferability of the result, as they might be specific to Zurich and that the results are not independent of demand changes.

Nagle and Gayah (2014) followed up on the idea of using mobile probes in estimating traffic states. The MFD is not known a-priori. The paper first sets up some traffic metrics based on the Edie's generalized traffic definitions[1] to be estimated with mobile probes and goes on to postulate the variance thereof depending on the penetration rate. The penetration rate is estimated, by taking

[1] Edie's generalized traffic definitions are fundamental for the understanding of traffic flow and can be looked up in almost any book treating traffic flow, such as (Hall, 2012).

the ratio of the number of probes and the number of total vehicles in the system. The number of mobile probes could be evaluated with the help of loop detectors by tracking the mobile probes (e.g. GPS) when passing at loops. The authors thereby assume that enough loop detectors are detecting mobile probes over a long enough observation period to estimate the penetration rate accurately. A micro simulation of a grid with one-way streets is carried out in order to verify the variance of the traffic metrics based on different penetration rates. MFDs are estimated at different penetration levels, and their accuracy is evaluated with the use of a root mean squared errors. The results are in accordance with the previous study (Gayah and Dixit, 2013): Increasing the penetration level of mobile probes, increases the accuracy. Concluding, the authors of the study remark that a penetration rate of 0.2 leads to estimates of flow and density within 10% of the true value.

Leclercq et al. (2014) presented a cross-comparison of link data and probe data. Among its contribution is a correction method for densities of links, improperly measured by loop detectors - which is the aforementioned deficit of loop detectors, treated by Buisson and Ladier (2009) and by Courbon and Leclercq (2011) (cf. section 2.2). The authors show with traffic flow theory a significant improvement that can be provided for an urban corridor. However, the method still needs further development for an urban network. It is suggested to use speed estimates from floating car data and use flows from loop detectors to estimate the MFD is introduced. However, since the basic procedure to estimation an MFD is the same as Gayah and Dixit (2013) used, the same limitations are valid: A well-defined MFD must be known and the accuracy achieved is insufficient.

Nagle and Gayah (2015) compared the use of data coming from fixed detectors and mobile probe data for perimeter control. In a micro simulation of a grid with one-way streets with a simple perimeter control, the MFD is estimated based on link and probe data according to the methods proposed by Geroliminis and Daganzo (2008) and Gayah and Dixit (2013), respectively. In a first experiment without any perimeter control, the estimated density from fixed detectors was consistently higher than from probe data for the same time step. The loop detectors were placed in the middle of each link, thereby overestimating density (cf. (Buisson and Ladier, 2009)). The second experiment was carried out with perimeter control, but without accounting for any uncertainty due to a small subset of links or due to a low level of penetration rate. A perimeter control was activated if the estimated density was higher than the critical density. Delay savings are taken as a proxy for how well the perimeter control operates. When comparing different subsets of links (loop detectors) or different penetration levels (mobile probes) the average delay savings do not significantly differ from the average delay savings obtained with 100% of the links or a penetration rate of 1, respectively. In other words, even if 5% of the links make up the subset of links monitored, the average delay savings is approximately the same as if 100% of the links were monitored. Finally, the third experiment incorporated an uncertainty due to a small subset of links or due to a low level of penetration rate. The authors conclude that informing the perimeter control using only a subset of links or vehicle is feasible. As limitation to the study, the uniform demand assumption was noted.

3 Methodology

As pointed out in chapter 2, a study of the literature about the macroscopic fundamental diagram (MFD) reveals that the two main traffic data sources, loop detectors and floating car data have been analyzed *separately*, and compared with each other, also in respect to the network coverage. However, in most cities, loop detectors and floating car data (for example from cell phones or from GPS devices) co-exist. The novelty of the methodology introduced in this section lies in the approach to *simultaneously* use the two data sources, by the means of a data fusion. The advantage of such an approach is that with a fusion the MFD is possibly more accurate than if only one data source were used. In order to investigate possible benefits of a fusion the experimental setup described in the following sections was used.
The following gives a brief outline of the experimental setup:

1. Perform a micro simulation of traffic in a grid network. Thereby all vehicles in the network are tracked. See section 3.1.

2. Use the traffic micro simulation output to simulate floating car and loop detector data with different levels of network coverage (for example, 10% of the vehicles serve as mobile probes and 20% of links have loop detectors installed). See section 3.2.

3. Propose fusion methods and assess the MFD estimation thereof. See sections 3.3, 3.4 and 3.5.

3.1 Traffic Simulation

Network Layout A grid network is used, and constructed in VISSIM, a product of the German PTV group. The network consists of a one-way network constructed by Ortigosa et al. (2015). The network is a 10 by 10 grid with 180 main links, each 120 m long and each having two lanes, (cf. fig. 2). The direction of travel for the one-way link is opposite to the neighboring, parallel links. In other words, every other, parallel link has the same direction of travel. 1524 smaller links and connectors were also in the network, their use, however, was only to "connect" the main links. Thus, they were excluded from further analysis.

Simulation Period, Resolution and Randomness All simulations were run for 1 hour simulation time during which, the demand was constant. The simulation resolution was set to 2Hz, e.g. every half second, the simulation recorded the values mentioned in the following. Five different random seeds were used (random seed 42-46).

Vehicle Composition Traffic in the simulations consisted of cars with default VISSIM behavior only (cf. (PTV, 2014)).

Traffic Demand In the middle of each of the 180 main link, a "demand node" is placed, which was used to produce and attract cars in the network - it acts as an origin and destination node. The demand nodes are constructed with the

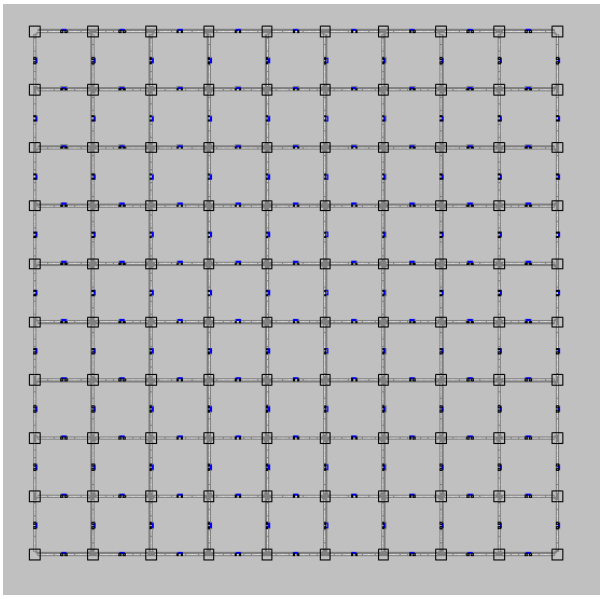

Figure 2: Snapshot of the network layout used in VISSIM.

help of parking lots serving as zone connectors - no delays are induced when vehicles enter the network to other vehicles in the network. (PTV, 2014)
A uniform demand throughout the network is ensured by having all demand nodes producing and attracting cars with the same probability. In other words, for a standardized case: all links have a demand node, which produces 1 vehicle for each of the remaining 179 links to attract during a period of 1 hour - in this case, a total of 32'220 vehicles (179x180) would theoretically reach their destination. In order to have a full coverage of the MFD, demands were chosen to range from 0.3 to 0.6 times the standardized case, resulting in a demand range of 9'666 to 22'554 trips an hour.
A more realistic loading of the network could have been achieved by loading the demands one after the other in an interval of 1 hour and let the simulation run for 4 hours. However, the large amount of data that would have been created that way (all vehicles tracked at 2Hz), made it impossible to carry out the more realistic loading of the network.

Traffic Assignment The routes are assigned dynamically, according to the built-in dynamic traffic assignment (DTA) module in VISSIM, which follows roughly a user equilibrium principle. In order to converge to a stable solution the module implements an iterative process, where the utilities of the different routes are calculated and the new routes are found by using a altered form of the method successive averages (MSA). For the simulations, a moderate Kirchoff parameter of 5 was chosen. It indicates how sensitive people are to a route not being the shortest (Ortigosa et al., 2015). The route choice is updated every half hour (according to the recommendation by PTV (2014)). A convergence criteria was set to 5%, i.e. when the individual travel time on the routes do not differ

more than 5% from previous iterations. In average around 15-20 iterations were needed to find convergence. Further details can be found in (Ortigosa et al., 2015) and (PTV, 2014).

Traffic Operations At each intersection, a traffic light was set to a 60 seconds cycle length, with 27 seconds of green for turning and through traffic and 3 seconds lost time, at the change of each phase. There was no phase shift between up- or downstream traffic lights.

Output The output of the simulation is VISSIM's "vehicle record", which records the cumulative time and cumulative distance traveled in the system of each vehicle, as well as the link's identification number on which it is traveling. Additionally, the simulation time and the car's identification number are recorded. This builds the foundation of the mobile probe data set. The amount of data collected for the vehicle record can easily reach some 30 millions of rows in data, since all of the mentioned variables are tracked on a 2Hz resolution.

3.2 Building the MFD

This section gives an overview of the methodology used to create MFDs from VISSIM's output described in subsection 3.1.

In order to calculate the points of the MFD, the weighted flow and density averages across all links in the network are used. A point in the MFD is defined by an average weighted flow, and an average weighted density (cf. section 2.2). These average flows $q_{t,MFD}$, and average densities, $k_{t,MFD}$, are obtained for every time slice t, e.g. every 5 minutes. q_t^i and k_t^i correspond to the flow and density of link i for time slice t, and l^i corresponds to the length of link i (multiplied with the number of lanes).

$$q_{t,MFD} = \frac{\sum_i q_t^i l^i}{\sum_i l^i} \qquad k_{t,MFD} = \frac{\sum_i k_t^i l^i}{\sum_i l^i} \tag{1}$$

Since in the presented network all links have the same length, eq. 1 can be simplified to the following.

$$q_{t,MFD} = \bar{q}_t \qquad k_{t,MFD} = \bar{k}_t \tag{2}$$

where $\bar{q}$ and $\bar{k}$ are the *average* volume and density in the network. When dealing with FCD the approach by Nagle and Gayah (2014) can be applied directly to calculate the average flow and density based on Eddie's generalized definitions (cf. (Hall, 2012))..

$$q_{t,MFD} = \bar{q}_t = \frac{d_{tot,t}}{LT} \qquad k_{t,MFD} = \bar{k}_t = \frac{t_{tot,t}}{LT} \tag{3}$$

where q and k are the the flow and density measured in the network, respectively. d_{tot} and t_{tot} are the *total distance* and the *total time* traveled in the system. L and T are the length of the examined network or sub-network and

the time of observation (e.g. 5min).

The following explains how floating car data and loop detectors are simulated at different levels of network coverage, based on the output of the micro simulation.

Floating Car Data With the output of VISSIM, all vehicles are tracked on all links. This makes creating floating car data simple. Some cars are flagged as *mobile probe vehicles* - they send their time and distance spent in the network and based on Edie's generalized definitions, it is then possible to calculate flow and density, two variables needed for an MFD (cf. eq. 3).

Loop detectors Creating loop detector data is more complicated. Loop detectors usually measure flow and occupancy, where latter can be converted to density. However, this density depends on the placement of the loop within the link (cf. section 2.3), making an accurate mimicking with VISSIM's output difficult. This effect can be neglected, under the assumption that loop detectors are well distributed within the links (i.e. in one link the loop detector is placed close to the intersection, in another link it is placed further upstream, etc.). The *aggregated* measurements will be close to the average real value, which would be measured by a "perfect" loop detectors (Courbon and Leclercq, 2011). This consideration applies to the MFD since it is a macroscopic (i.e. aggregated) method. In other words, for this simulation, loop detectors are able to measure correctly flow and density for the whole link (analogue to Ortigosa et al. (2014)). Therefore, analogue to the floating car data it is possible to mimic "perfect" loop detectors: A loop detector on a specific link is created by using the time and distance spent of all vehicles on this specific link to calculate flow and density based on Edie's generalized definitions.

Network coverage It is of interest how well the MFD can be estimated with only limited information. Therefore a setup is created that keeps only information of certain vehicles and links. Let's say an exemplary network has 100 links with 500 cars circulating on them. The idea is to investigate how well the network can be described with relying on only 3 loop detectors installed in 3 links and getting GPS information of 50 cars traveling in the network. In other words, the network has a *link surveillance rate* of 3%[2] and a mobile *probe penetration rate* of 10%. There are many different possibilities on how to chose 3 links out of network with 100 links[3]. In order to increase statistical representativeness, 1000 combinations for each link surveillance rate are tested. Applied on the example, different combinations of 3 links are chosen 1000 times, over and over again. The procedure is analogue for the mobile probes.

Implementation The following shows how the MFD calculations are implemented. The programming language R is used to perform the calculations.

[2]If links are not equidistant, the length of the link should also be taken into account.
[3]There are 161'700 possibilities.

1. **Aggregation**: Aggregate vehicle record data in *300s time intervals*, in respect to distance and time traveled. This is performed for each vehicle (data used for mobile probes) and for each link (data used for loop detectors). The first 300s of a simulation were considered as warm-up and thus excluded from analysis.

2. **Create subsets**: A total of 30 *probe penetration rates* and *link surveillance rates* were chosen from the same set, $\{1/30, 2/30, \ldots, 1\}$. As there are 180 links in the network, 30th quantiles ensure integer number of links being chosen.

    - Set a probe penetration rate, by randomly assigning vehicles as mobile probes (subset). The method allows using one simulation from VISSIM to set different levels of probe penetration rates without actually having to run a simulation with a certain level of mobile probes. 1000 different random seeds were employed to create the subsets. The probe penetration rate is defined as $\rho = \frac{N_p}{N_{tot}}$, where N_p is the number of probes and N_{tot} is the number of total vehicle in the network. The probe penetration rate is set over a duration of 3300s[4]. Further details in section 3.3.
    - Set a link surveillance rate by keeping only observations that pass over a certain subset of links, independent of them being mobile probes or not. Again, 1000 different random seeds were employed to create the subsets.

3. **Calculation**: Calculate the average flow and density in the network with Edie's generalized definition taken from (Nagle and Gayah, 2014), for loop detectors and for mobile probes. Further details in section 3.5.

4. **Fusion**: Fusing the results from loop detectors and from probe data. Further details in section 3.5.

5. **Comparison**: Analyze the accuracy of the estimated MFD compared to the real MFD. Further details in section 3.4.

3.3 Estimation of Probe Penetration Rate

In reality the mobile probe penetration rate is usually not known. In the two following subsections, the estimation of the probe penetration rate in the network is explained.

3.3.1 Probe Penetration Rate Known a-priori

When all links in a network are used to estimate the probe penetration rate, then: $\hat{\rho} = \frac{N_p}{N_{tot}} = \rho$, where $\hat{\rho}$ is the estimated penetration rate and ρ is the probe penetration rate. If N_p and N_{tot} are known, then the probe penetration rate is known a-priori. Strictly spoken, when the exact probe penetration rate is known a-priori, no estimation of the probe penetration rate takes place.
In some cases, the probe penetration rate might be known in reality. For example, if the mobile probe data is generated by mobile phones of one carrier, then

[4] 3600s - 300s warm-up

the market share of that carrier could serve as probe penetration rate, assuming that its phone users are distributed homogeneously in traffic.

3.3.2 Probe Penetration Rate not Known a-priori

When the probe penetration rate is not known a-priori, a combination of vehicle trajectories and loop detectors are used to estimate the probe penetration rate. Loop detectors recognize all vehicles, independent of them being a probe or not. Probe vehicles register their link trajectory. Therefore, the probe penetration rate can be estimated by dividing the number of probe vehicle passing on a certain link by the count of all vehicles that pass over that certain link with an installed loop detector. In short, $\hat{\rho} = \frac{N_{p,lsr}}{N_{tot,lsr}}$ with $N_{p,lsr}, N_{tot,lsr}$ being the number of probes and total number of vehicles counted on the specified subset of links. The index *lsr* indicates that only a certain subset of links in the network are used to count the number of probes and the total number of cars.

The same links that are incorporated to estimate the MFD parameters by loop detectors are incorporated to estimate the probe penetration rate. That is to say, if the network has a link surveillance of 10%, then these 10% links will be used to estimate the probe penetration rate. This estimation method follows the outline by Nagle and Gayah (2015).
As seen in section 3.2, the probe penetration rate is set over the length of one VISSIM simulation, 3300s. However, the probe penetration is estimated every 300s.

For further discussion and analysis, the following definitions are introduced:

- The *set probe penetration rate (sppr)*, the probe penetration rate that is set over a period of 3300s. It is used if the probe penetration rate is known a-priori.
- The *true probe penetration rate (tppr)*, which stands for the real probe penetration rate during the 300s period. It can be calculated, if all links in the network are taken into account (i.e. a link surveillance rate of 100%).
- The *estimated probe penetration (eppr)*, the probe penetration rate that is estimated over a period of 300s by using the method mentioned above. However, only a subset of links is used (i.e. a link surveillance rate smaller than 100%).

The estimated and the true probe penetration rate do not have to be identical - the true probe penetration rate tends to vary somewhat around the set probe penetration rate. An example sums up: Let's say, the set penetration rate is 0.2. During a period of 300s, 10% of the links equipped with loop detectors calculate the estimated probe penetration rate to be 0.25. But if all links were equipped with loops and were taken into account to measure the probe penetration rate, we would get 0.22, which is the true probe penetration rate.
It is of interest, how well a certain level of link surveillance can estimate the true probe penetration rate. Therefore, the following methodology based on the relative errors is introduced.

$$relative\ error = \frac{|eppr - tppr|}{tppr} \tag{4}$$

An experimental setup estimating the probe penetration with different probe penetration and link surveillance rates was carried out. Thereby the subsets for different probe penetration and link surveillance rates were randomly chosen 1000 times (for more details, see section 3.2).

3.4 Accuracy of an Estimated MFD

When an MFD is estimated with incomplete information (e.g. only 10% of the vehicles are equipped with GPS), different approaches can be taken to evaluate its accuracy. Let MFD stand for the real MFD, which can be calculated with full network coverage, and eMFD for the estimated MFD, which is calculated when the network has incomplete coverage (e.g. only 10% of the vehicles are equipped with GPS). Two approaches are formulated:

- The **sum of the relative errors** of the density and the volume estimates. This is an alternation of the method proposed by Nagle and Gayah (2014), where each error was shown on its own.

$$\Delta S_t(MFD, eMFD) = \frac{\Delta q_t}{q_{real,t}} + \frac{\Delta k_t}{k_{real,t}} \tag{5}$$

$$\overline{\Delta S} = \frac{1}{m_t} \sum_t \Delta S_t(MFD, eMFD) \tag{6}$$

  where Δ is the absolute difference between the estimate and the real value for a time slice t. And, m_t is the total number of time slices considered, which is identical for the eMFD and the MFD. This leads to the average sum of the relative errors, $\overline{\Delta S}$, which has the units percentage points (ppts).

- The approach of **Ortigosa et al. (2014)** where the error is in respect to the critical density. Thereby it is differentiated between the congested and the uncongested branch of the MFD.

$$\Delta R_t(MFD, eMFD) = \begin{cases} \frac{k_t - k_{cr}}{k_{cr}} - \frac{k'_t - k'_{cr}}{k'_{cr}} & \text{if } k_t < k_{cr} \\ \frac{k_t - k_{cr}}{k_j - k_{cr}} - \frac{k'_t - k'_{cr}}{k'_j - k'_{cr}} & \text{if } k_t > k_{cr} \end{cases} \tag{7}$$

$$\overline{\Delta R}(MFD, eMFD) = \frac{1}{m_t} \sum_t |\Delta R_t(MFD, eMFD)| \tag{8}$$

  where k'_t and k_t stand for a density point in the eMFD and MFD, respectively, for a time slice t, k'_{cr} and k_{cr} stand for the critical density for the eMFD and MFD, respectively, and k'_j and k_j stand for the jam density for the eMFD and MFD, respectively. The critical density is approximated by taking the average density of the top 3 values of flow. The jam density is approximated by taking the average of the top 3 values of density. This slight alteration compared with (Ortigosa et al., 2014), where the top 1% flow values are averaged, is due to the fact that an MFD for 1 random seed is composed of 44 points (cf. section 4.2).
  The average over time is $\overline{\Delta R}$ calculated with m_t, which is the total number of time slices considered, which is identical for the eMFD and the

MFD. The units of $\overline{\Delta R}$ are percentage points (ppts). This method has the advantages, 1) that it does account for the triangular shaped form of the MFD by taking the relative errors with respect to the critical density (unlike the aforementioned error which takes the y-axis as a reference line for the errors in density), and 2) that it is a more efficient way of determining, how well an estimated MFD can be used for a perimeter control solution (see sections 2.2 and 2.3 for perimeter control). Contrary to the sum of the relative errors, it does not take volume measurements into account (except for the calculations of the top flow).

3.5 Fusion Methods

The complexity of a possibly beneficial fusion for the MFD lies in the non-linear way, how traffic congestion distributes in a network. A fusion needs to be capable to bring benefits to a network estimation when congestion is non-existent (uncongested branch of the MFD) and also when congestion is heavy and (extremely) heterogeneously distributed (congested branch of the MFD).
Furthermore, the data coming from mobile probes and from the loop detectors are "competitive", i.e. they measure the same parameters of the identical network (Mitchell, 2007): Having 100% of the loop detector data, will lead to a state of perfect information, where the MFD can be fully estimated. Adding data from mobile probes with a probe penetration rate throughout the network of, say, 40% will worsen our estimation of the traffic state, since we would fuse complete data with incomplete data. Thus, more data does not automatically lead to better estimations. The floating car data and the loop detector data represent the identical network with the identical set of vehicles, so taking more data does in some cases not lead to better estimations.

In the following subsections, 6 different methods are presented, on how to estimate the MFD based on loop detectors and mobile probe data.
As described in section 3.2 there are 30 levels of link surveillance and 30 levels of probe penetration rates implemented. To evaluate the benefits of a fusion the 30 levels of link surveillance are cross joined with 30 levels of probe penetration rates, resulting in 900 combinations of network coverage[5]. In order to increase statistical relevance, each combination of network coverage was created 1000 times with different subsets. An example for 1 network coverage combination to clarify: A given network with 100 links and 500 cars circulating on it is investigated. Analogue to the example in 3.2, 3 links have a loop detector and 50 vehicles can be tracked. It is now of interest, how well this specific combination can estimate the MFD. For the statistical representativeness, different combinations of 3 links and different combinations of 50 vehicles are chosen 1000 times - creating 1000 eMFDs with the same network coverage combination. Therefore, a total of 900'000[6] different eMFDs are compared to 1 real MFD .
Furthermore the proposed fusion methods are investigated for two cases: 1) Knowing the probe penetration rate a-priori, 2) not knowing the probe penetration rate a-priori (cf. section 3.3). When the probe penetration rate is not

[5] Method 0 builds an exception since it does not fuse any data.
[6] 30 link surveillance rate x 30 probe penetration rate x 1000

Table 1: Proposed fusion methods in an overview.

Method	Methodology
0	No fusion.
1	Fuse according to network coverage and accuracy of each source.
2	Fuse according to the network coverage of the loop detectors.
3	Fuse according to the network coverage of the loop detectors and the accuracy of floating car data.
4	Fuse according to the number of observations contributed by each source.
5	Estimate flow values from loop detectors only; estimate density values from mobile probes only.

known it is estimated with the loop detectors in the network. In this case, an MFD estimation based solely on mobile probes is impossible: If no loop detector is available to estimate the probe penetration rate, then the mobile probes cannot estimate an MFD with any of the proposed methods.

Table 1 gives an overview of the fusion methods, which are discussed in the following.

3.5.1 Method 0

The simplest method to create an eMFD is taking data from each source separately, e.g. calculating the density and flow values only based on mobile probes or only based on loop detectors. This method follows the schemes introduced by Nagle and Gayah (2014) and Nagle and Gayah (2015). No fusion of the data is performed. In this case, the probe penetration rate is not estimated - it has to be known a-priori.

$$\hat{q} = \begin{cases} \frac{D_p}{\rho LT} & \text{for probes} \\ \bar{q}_{loops} = \frac{D_l}{\phi LT} & \text{for loops} \end{cases} \qquad \hat{k} = \begin{cases} \frac{T_p}{\rho LT} & \text{for probes} \\ \bar{k}_{loops} \approx \frac{T_l}{\phi LT} & \text{for loops} \end{cases} \tag{9}$$

where D_p, D_l and T_p, T_l stand for the total distance and the total time traveled by the mobile probes (subscript p) or the total distance and total time traveled by all vehicles on the selected subset of links (subscript l), respectively, ρ stands for the probe penetration rate known a-priori and ϕ for the link surveillance rate. L and T stand for the total length of the network and observation time, respectively.
For mobile probes the eq. 9 follows the approach of taking all mobile probes in the network and calculating the density and the flow thereof. For loop detectors, the findings of Courbon and Leclercq (2011) are used. In other words, the average density measurement of loop detectors well distributed within the links is approximately accurate, meaning it corresponds to the density calculated with Edie's generalized formula (cf. section 3.2). Flow is measured accurately by loop detectors.

3.5.2 Method 1

According to method 0, the network's parameters can be estimated by using only link data or only mobile probes. An intuitive approach is a proportional weighting relative to the levels of information of the two sources, loop detectors and mobile probes. Meaning, if the link surveillance is 20% and the probe penetration rate is 10%, then the results of the loop detectors would be weighted twice and the results from the probes once. The drawback of such a weighting method: Taking data from a link surveillance rate of 100% and a probe penetration rate of 50%, would also lead to having the results from the loop detectors weighted twice and the results from the probes once. This would mean that we worsen a state of perfect information (100% of link surveillance) by adding imperfect information (50% probe penetration).
Thus, the "accuracy" of a certain link surveillance or probe penetration should be taken into account. This alters the aforementioned weighting by multiplying it with $\frac{1}{1-\rho}$ (factor for loops is analogue with ϕ instead of ρ). Thereby it takes into account that data from a probe penetration of for example 90% are more reliable than data from a probe penetration of 1%.

$$\tilde{q} = \begin{cases} \dfrac{\frac{1}{1-\rho}\rho\hat{q_p} + \frac{1}{1-\phi}\phi\hat{q_l}}{\frac{1}{1-\rho}\rho + \frac{1}{1-\phi}\phi} & \text{if } \rho < 1 \wedge \phi < 1 \\ \hat{q_p} & \text{if } \rho = 1 \\ \hat{q_l} & \text{if } \phi = 1 \end{cases} \tag{10}$$

$$\tilde{k} = \begin{cases} \dfrac{\frac{1}{1-\rho}\rho\hat{k_p} + \frac{1}{1-\phi}\phi\hat{k_l}}{\frac{1}{1-\rho}\rho + \frac{1}{1-\phi}\phi} & \text{if } \rho < 1 \wedge \phi < 1 \\ \hat{k_p} & \text{if } \rho = 1 \\ \hat{k_l} & \text{if } \phi = 1 \end{cases} \tag{11}$$

where $\tilde{q}$ and $\tilde{k}$ refer to the estimated network flow and network density based on the data fusion. All other variables are defined in eq. 9. The denominator ensures that the weight ranges between 0 and 1. A probe penetration rate of nearly 100% leads to a weight of 1 for the data coming from probes, and makes the link data oblivious with a weight of 0. Vice versa holds true in the case of a link surveillance rate of 100%. If the link surveillance rate or the probe penetration rate is 0 ($\phi = 0$ or $\rho = 0$), no fusion takes place. In that case the density and the flow is estimated with the other source only.
If the probe penetration rate needs to be estimated, ρ becomes $\hat{\rho}$ (also for eq. 9).

3.5.3 Method 2

A drawback of method 1 is that it does not take into account that a loop detector on one link uses information from all cars on this specific link, contrary to mobile probes over that link. When looking at link level, it can be postulated: For all links with a loop detector, adding data from mobile probes cannot improve the

accuracy.
Knowing that all links in the grid network have the same length, the proposed method is as follows.

1. For each link: If loop detectors exists, use only loop detector data, if no loop detectors, use mobile probe data.

2. Calculate the average volume and density for the two subsets in the network (sub-network with loop detectors and sub-network without loop detectors).

3. Weight the two averages with ϕ and $1-\phi$ respectively, with ϕ being the link surveillance rate.

In short:

$$\tilde{q} = \begin{cases} \phi\hat{q}_l + (1-\phi)\hat{q}_{p-l} & \text{if } \rho > 0 \\ \hat{q}_l & \text{if } \rho = 0 \end{cases} \quad \tilde{k} = \begin{cases} \phi\hat{k}_l + (1-\phi)\hat{k}_{p-l} & \text{if } \rho > 0 \\ \hat{k}_l & \text{if } \rho = 0 \end{cases} \tag{12}$$

with an alteration to eq. 9:

$$\begin{aligned} \hat{q}_l &= \frac{D_l}{\phi LT} && \text{for subnetwork with loop detectors} \\ \hat{q}_{p-l} &= \frac{D_p}{\rho(1-\phi)LT} && \text{for subnetwork without loop detectors} \\ \hat{k}_l &= \bar{k}_{loops} \approx \frac{T_l}{\phi LT} && \text{for subnetwork with loop detectors} \\ \hat{k}_{p-l} &= \frac{T_p}{\rho(1-\phi)LT} && \text{for subnetwork without loop detectors} \end{aligned} \tag{13}$$

$\hat{q}_l$ and $\hat{k}_l$ are now the average volume and density measured on links with loop detectors, respectively (same as in eq. 9). $\hat{q}_{p-l}$ and $\hat{k}_{p-l}$ stand for the average volume and density measured from mobile probe data according to the above equations, on links with no loop detectors. ϕL stands for the length of the sub-network with loop detectors on links and $(1-\phi)L$ stands for the length of the sub-network without loop detectors. If the link surveillance rate or the probe penetration rate is 0 ($\phi = 0$ or $\rho = 0$), no fusion can take place. In that case the density and the flow is estimated with the other source only.
If the probe penetration rate needs to be estimated, ρ becomes $\hat{\rho}$.

3.5.4 Method 3

A drawback of method 3 is that it does not take the mobile probe penetration rate into account. In other words, if 20% of the links are surveyed by a loop detectors ($\phi = 0.2$), then the 80% rest of the network that are covered with mobile probes are weighted with 0.8, independently if the probe penetration is 99% or 1%. Thus, it makes sense to discount the weight of the data coming from mobile probe as a function of their accuracy. If the probe penetration rate is low, the accuracy is low as well (cf. section 2.3).
This leads to the following weighting based on method 2 (especially, eq. 13).

$$\tilde{q} = \frac{\phi\hat{q}_l + \sqrt{\rho}(1-\phi)\hat{q}_{p-l}}{\phi + \sqrt{\rho}(1-\phi)} \quad \tilde{k} = \frac{\phi\hat{k}_l + \sqrt{\rho}(1-\phi)\hat{k}_{p-l}}{\phi + \sqrt{\rho}(1-\phi)} \tag{14}$$

Multiplying the weight of the mobile probe data with square root of ρ ensures that lower probe penetration rates with high inaccuracy are not taken too strongly into account. For illustration, take the above example with a $\phi = 0.2$ $\rho = 0.01$, the weight of the mobile probe data changes from 0.8 (method 2) to $\frac{0.8 \cdot \sqrt{0.01}}{0.2 + \sqrt{0.01} \cdot 0.8} = 0.29 < 0.8$. If the link surveillance rate or the probe penetration rate is 0, no fusion takes place. In that case the density and the flow is estimated with the other source only.
If the probe penetration rate needs to be estimated, ρ becomes $\hat{\rho}$.

3.5.5 Method 4

Method 4 uses the same data collection setup as method 2 and 3, where probe data is only taken into consideration when there are no loop detectors. In contrary to the aforementioned methods 2 and 3, this method incorporates absolute numbers. The averages of the sub-networks from eq. 13 are weighted according to their number of observations. In short:

$$\tilde{q} = \frac{N_l\hat{q}_l + N_p\hat{q}_{p-l}}{N_l + N_p} \tag{15}$$

$$\tilde{k} = \frac{N_l\hat{k}_l + N_p\hat{k}_{p-l}}{N_l + N_p} \tag{16}$$

where N_l is the number of observations over links with static surveillance and N_p is the number of observations registered on links with no loop detectors. If the link surveillance rate or the probe penetration rate is 0 ($N_l = 0$ or $N_p = 0$), no fusion takes place. In that case the density and the flow is estimated with the other source only.

3.5.6 Method 5

A method implied by Leclercq et al. (2014) is to use loop detectors to estimate the flow of the network and use the mobile probes to estimate the density of the network. The density estimated by loop detectors is possibly inaccurate (cf. section 2.3). It might therefore be reasonable to use only the density estimates of the mobile probe data. As in method 1, mobile probe data is used throughout the whole network (cf. 9).
In short:

$$\tilde{q} = \begin{cases} \hat{q}_l & \text{if } \phi > 0 \\ \hat{q}_p & \text{if } \phi = 0 \end{cases} \quad \tilde{k} = \begin{cases} \hat{k}_p & \text{if } \rho > 0 \\ \hat{k}_l & \text{if } \rho = 0 \end{cases} \tag{17}$$

where the $\hat{q}_l$ and $\hat{k}_l$ are defined in method 0. If the link surveillance rate or the probe penetration rate is 0, no fusion can take place. In that case the density and the flow is estimated with the other source only.

4 Results

4.1 Probe Penetration Rate

Fig. 3 shows, a contour plot of the 95th quantile relative error depending on the link surveillance and the probe penetration rate. It can be observed that, low levels of probe penetration benefit most from an increase in link surveillance, and vice versa. This is not astonishing, having only a few loop detectors makes the estimation more difficult. Having only a few cars being mobile probes makes it less likely that a loop detector detects a mobile probe, which in turn, makes the estimation more difficult.

Fig. 4 shows the variance of the true probe penetration rate (tppr) for certain set probe penetration rates. As noted in (Nagle and Gayah, 2014) the variance follows a quadratic function: When setting the probe penetration over a period of 3300s and estimating it over a period of 300s, the estimates follow a binomial distribution, every vehicle has the same chance of being a probe vehicle. The variance of a binomial distribution is proportional to $p(1-p)$, where p is the probability (here: the probability of being a probe vehicle), explaining the quadratic curve. This indicates that the method creating subsets and estimating the probe penetration rate presented in sections 3.2 and 3.3 indeed follow the outlines presented by (Nagle and Gayah, 2015).

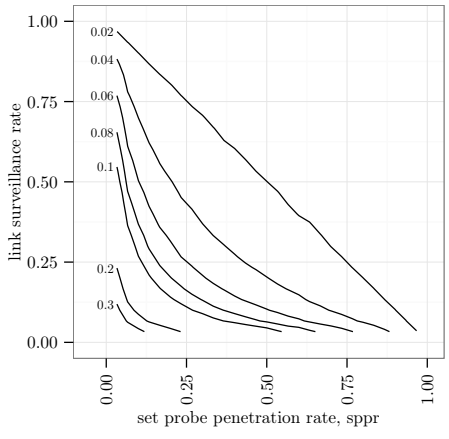

Figure 3: Relative error of probe penetration rate estimation.

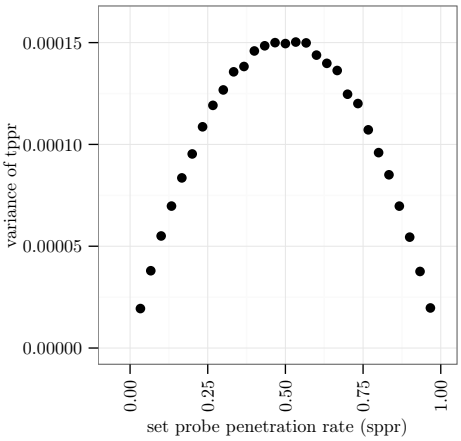

Figure 4: Variance of tppr.

4.2 Real MFD

Assuming that every link can be surveyed or that every vehicle's trajectory can be recorded, a real MFD can be calculated according to section 2.2 and eq. 3. This MFD is called real since it represents the MFD that can be observed with full information. As already mentioned multiple times, this MFD is practically impossible to observe in reality. In fact, in reality only certain links have loop detectors, and only a certain (time-variable) portion of vehicles are capable of

serving as mobile probes.

Fig. 5 shows the MFD for the network explained in section 3.1, split in demands (0.3-0.6 of the standardized case) and random seed (42-46). The typical triangular form can be observed along with higher scatter in the congested branch of the MFD. Unsurprisingly, higher demand leads to more congestion. However, this MFD has a drawback leading to even more noise: It does not perfectly represent a continuous loading of the network, since each demand is run on its own, i.e. without any transition from 0.3 to 0.4 to 0.5 and to 0.6 (cf. section 3.1).

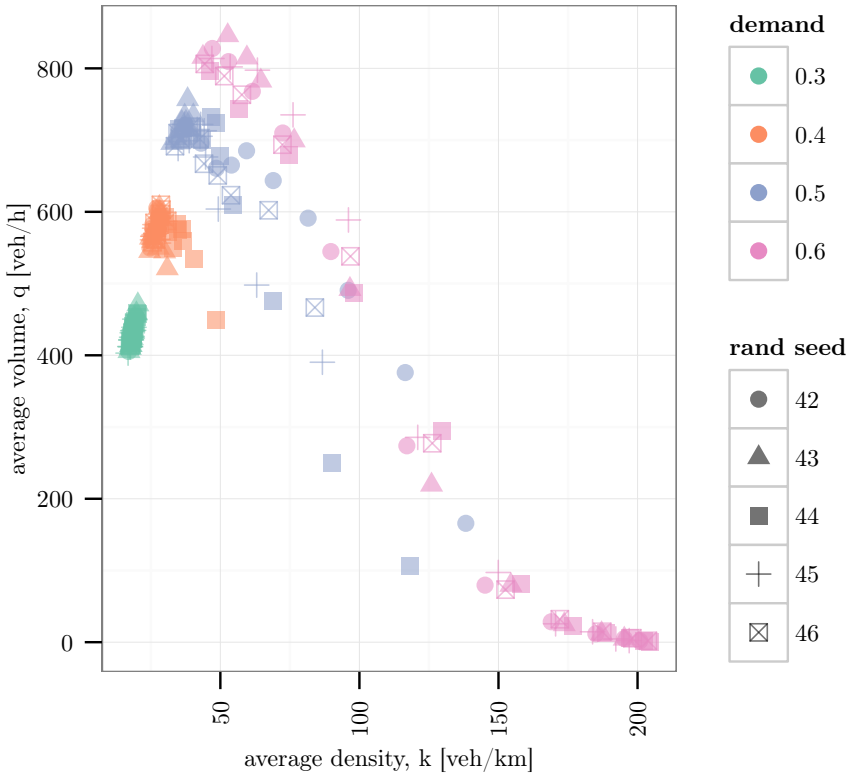

Figure 5: MFD with full network coverage.

4.3 Fusion Results

Almost all results shown in the next subsections show an "average 95th quantile error". This is an average value for the 5 different random seeds were used when simulating the network on VISSIM. In other words, for each combination of network coverage, the 95th quantile error is calculated out of the 1000 eMFDs created. Doing this for each of the 5 random seed of the VISSIM simulations gives 5 95th quantile errors. In the light of the amount of data processed, analysis shows that the 95th quantile error are all almost identical, which justifies

this simplification (cf. Annex). In other words, when interpreting a diagram, one can read: *"For 95% of the investigated cases, the error is smaller than the one reported in the diagram."*

4.3.1 Method 0

In fig. 6 the average 95th quantile of the errors of both methods are plotted against the network coverage. In other words, for 95% of the investigated cases, the error is smaller than the one reported in the diagram.
It can be observed that with increasing coverage of the network - by either increasing link surveillance rate or increasing probe penetration rate - the error decreases. For low network coverage, a sharp, almost parabolic, decline in errors can be registered when increasing low network coverage. Whereas increasing higher network coverage (>20%) does not decrease the errors by much. The marginal benefit (measured in a decrease of error) of adding network coverage decreases with increasing network coverage. Furthermore, both errors roughly follow the same trend, but the errors from Ortigosa et al. are always smaller than the error based on the relative error sum. The latter incorporates the volume's relative error as well. As can be seen in fig. 6, the errors for the

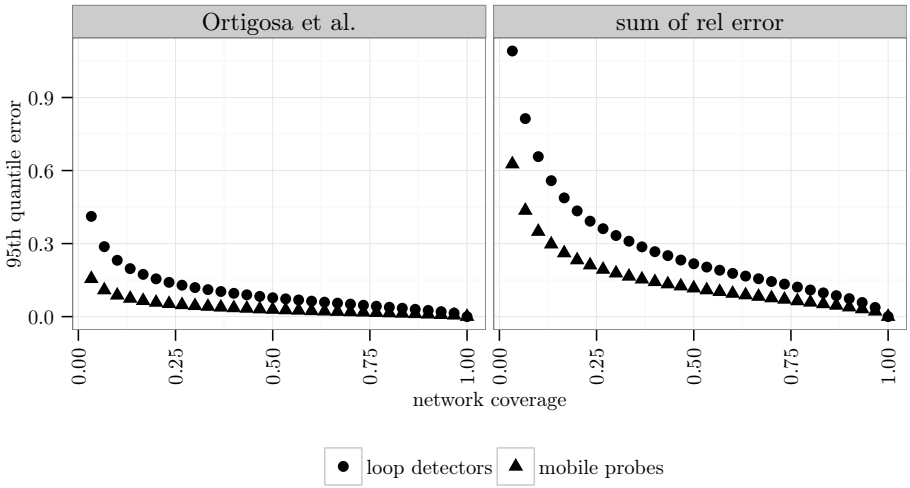

Figure 6: Average 95th error for mobile probes and loop detectors.

same network coverage is smaller when mobile probes are used. So, covering a network with mobile probes seems to be more effective than covering it with loop detectors.

It is of interest, how well mobile probes compared to loop detectors measure the state of the network. In order to compare both means of covering a network, the median error[7] per surveyed vehicle was calculated. A surveyed vehicle is a vehicle that either is a mobile probe or passed over a link with loop detectors. In fig. 7 the median errors of mobile probes per surveyed vehicle and of loop

[7] relative error sum

detectors per surveyed vehicle are taken as a ratio for each level of coverage and split up in demands (for VISSIM random seed 46)[8]. So, the median error per surveyed vehicle of the loop detectors at a 6% surveillance rate is divided by the median error per vehicle of the mobile probes at a penetration rate of 6%.
It can be observed that the higher the demand, the better the mobile probes measure in comparison to the loop detectors. As mentioned in chapter 2, the higher the demand, the higher the heterogeneity in the network. In other words, higher demands lead to a heterogeneous loading of the network, which is represented on the right branch of the MFD: Some links are heavily congested, others not. Mobile probes that are more or less evenly distributed in the network are better able to catch this high volatility, than trying to estimate the network with a limited amount of links surveyed. In fig. 7, a linear regression is added for each demand. Interestingly, the ratio of errors stays more or less the same. The advantage that mobile probes have over loop detectors are constant - even at 90% network coverage. Same holds true for comparing the two means of covering a network with the error after Ortigosa et al. (not shown).

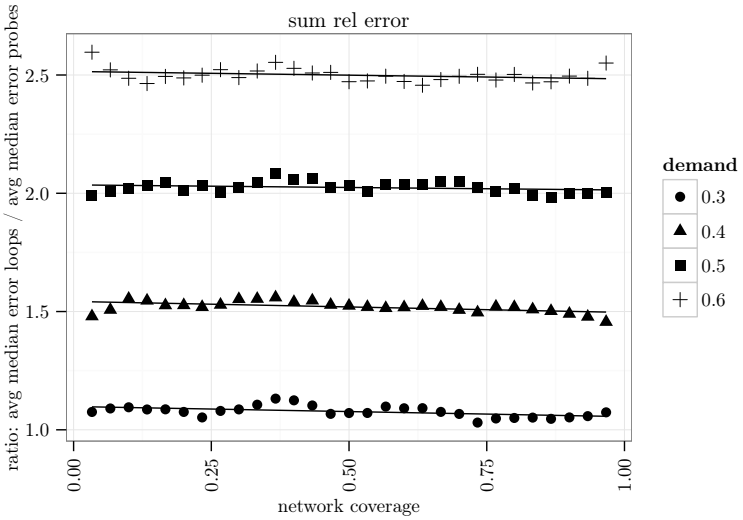

Figure 7: Ratio of the error measured by loops and the error measured by probes.

A comparison with median errors only - not weighted by surveyed vehicle - leads to the almost identical results as shown in fig. 7 (cf. annex).

4.3.2 Method 1

The results are shown in form of a contour plot: The x-axis corresponds to the probe penetration rate and the y-axis to the link surveillance rate. And the contour lines show the iso-error line, in other words, it connects all points with the same average 95th quantile error, based on the chosen fusion method. The darker lines indicate labeled intervals of 0.1[9] whereas the lighter ones indicate

[8] For the error calculations by demand, eq. 5 was used and not eq. 6.
[9] And also 0.05 is a darker line.

unlabeled intervals of 0.01.
In fig. 8 the contour plots for the fusion method 1 is shown, when probe penetration rates are known a-priori. Both error definitions are used (Ortigosa et al. and the sum of the relative errors). The errors shown for a probe penetration rate of 0 or a link surveillance rate of 0, represent the errors that would be measured if the data source were on its own.
Fusing data in this setup is only favorable, when levels of link surveillance are larger than probe penetration rates. If the link surveillance rate is smaller than than the probe penetration rate, a fusion of link data with probe data is not recommended, since the error increases at first. This is shown by a the leftward curve in the lower quarter of the diagrams. For the error after Ortigosa et al. this effect is even intensified. Generally, this is due to the lower level of accuracy coming from the loop detectors seen in method 0.

The higher the network coverage by either mobile probes or loop detectors,

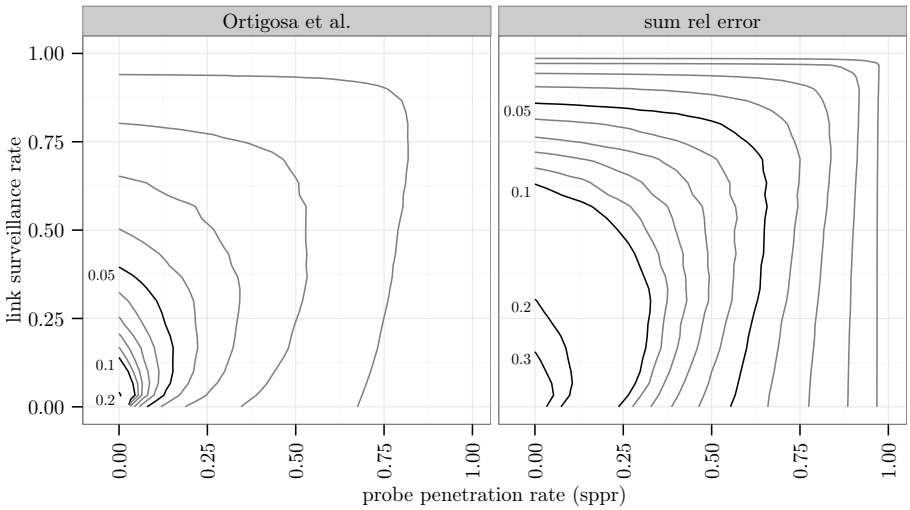

Figure 8: Contour plot of the average 95th quantile error for method 1 (sppr).

the less data fusion is beneficial. This can be attributed to: 1) the results of method 0, the errors of each source decrease quickly to remain low for higher levels of network coverage, thus it will not benefit from fusion so much; 2) the proposed fusion does not aim at fusing high levels of probe penetration with low levels of link surveillance and vice versa - the weight of data coming from 3% of the links is practically 0 (≈ 0.003) when the probe penetration rate is 90%.
In fig. 9 the contour plot is shown for a network where the probe penetration rate needs to be estimated, according to section 3.3. The difference lies also in the y-axis, which now stands for the estimated probe penetration rate.[10] In comparison to fig. 8, these results mostly differ for low levels of link surveillance

[10]In order to find the 95th quantile error, all estimated probe penetrations (eppr) were grouped in discrete 3% bins. This is necessary, because the estimated probe penetration rate is a continuous variable, unlike the set probe penetration (sppr). Discretization of the estimated probe penetration rate in intervals of 3% ensures that enough data is available to find a reliable 95th quantile. This was applied for all contour plots, where the probe penetration rate is estimated, in methods 1-5.

rates (smaller than 25%), because these cannot ensure an accurate estimation of probe penetration rate. In this (probably) more realistic setup, the fusion method is favorable for most combinations. Again, it is more favorable for combinations in the lower left quarter of the plot (ϕ and $\rho < 0.5$).

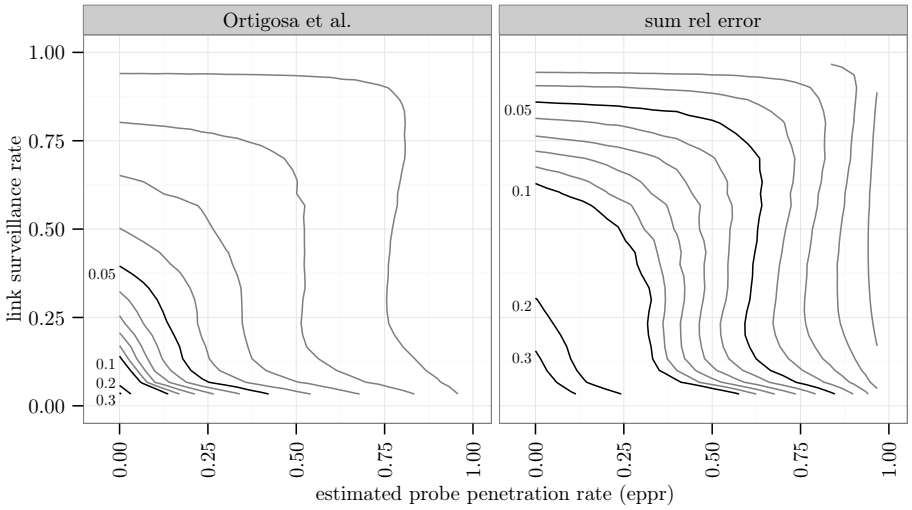

Figure 9: Contour plot of the average 95th quantile error for method 1 (eppr).

4.3.3 Method 2

The results are shown in the same form as for method 1 (for details, cf. 4.3.2). In fig. 10 the contour plots for fusion method 2 is shown, when probe penetration rates are known a-priori for both methods of error. The errors shown for a probe penetration rate or a link surveillance rate of 0, represent the errors that would be measured if the data source were on its own. In general, fusion based on this method is favorable. In most cases, fusing data with the other source, decreases the error. This holds true for low levels of link surveillance rates combined with any level of probe penetration rate (>25% of link surveillance rate). However, a tendency can be observed in which for low levels of probe penetration, a fusion is not recommended, since errors increase for low probe penetrations compared to no fusion at all. As mentioned earlier, the probe penetration levels are set at discrete values, the lowest being 1/30. However connecting the errors of a probe penetration rate of 1/30 and of 0 is not completely accurate: It is intuitive that, for probe penetrations even smaller than 1/30, the error would increase and to indicate this, the connecting iso-error lines are only dashed. The fact that no fusion for low rates of probe penetrations results in better results can be attributed to the weighting method: 1) According to equations 12f., a low link surveillance rate leads to a higher weight of the sub-network with no loop detectors ($1 - \phi$). And, low levels of probe penetration levels lead to inaccurate estimations. Together, too much weight is given to inaccurate estimations based on mobile probes. 2) the weighting method is discontinuous (with a case distinction). Both errors (Ortigosa et al. and sum of the relative

errors) differ almost only in magnitude.
In fig. 11 the contour plot[11] is shown for a network where the probe penetration

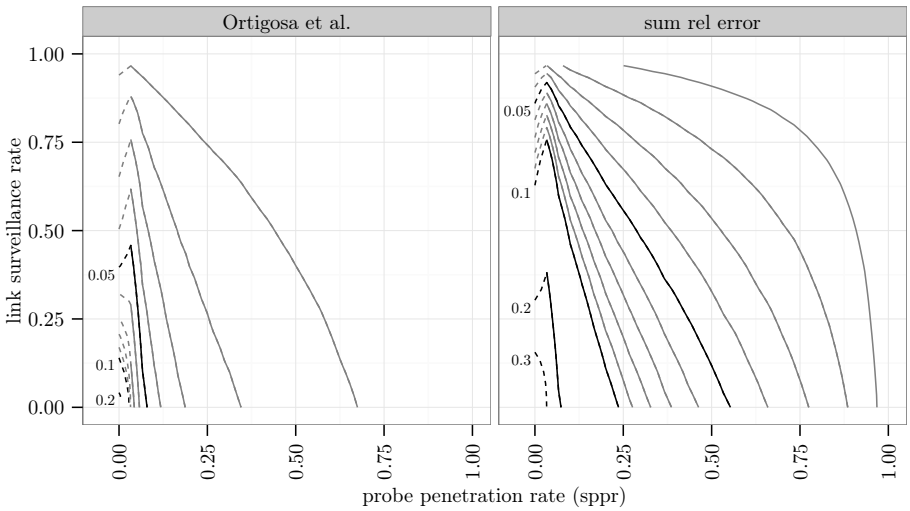

Figure 10: Contour plot of the average 95th quantile error for method 2 (sppr).

rate needs to be estimated, according to section 3.3. Compared to fig. 10, it differs mostly for low levels of link surveillance rates (smaller than 25%), because these cannot ensure an accurate estimation of probe penetration rate.
As a rule of thumb: Fusion method 2 can improve the estimation of the MFD, if the (estimated) probe penetration rate is higher than 10%.

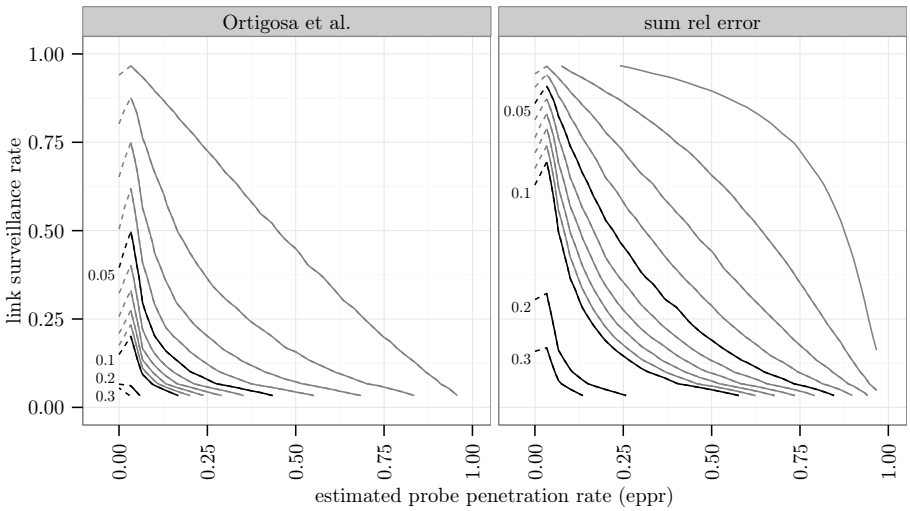

Figure 11: Contour plot of the average 95th quantile error for method 2 (eppr).

[11] See footnote 10

4.3.4 Method 3

The results are shown in the same form as for method 1 (for details, cf. 4.3.2). In fig. 12 the contour plots for the aforementioned fusion method is shown, when probe penetration rates are known a-priori. The errors shown for a probe penetration rate of 0 or a link surveillance rate of 0, represent the errors that would be measured if the data source were on its own. The plot shows that fusion with method 3 is always of advantage for the investigated combinations of network coverages. Discounting the weight of estimates based on mobile probes with the square root function proofs to be a suitable way of fusion. Both errors (Ortigosa et al. and sum of the relative errors) differ almost only in magnitude.

In fig. 13 the contour plot[12] is shown for a network where the probe penetration

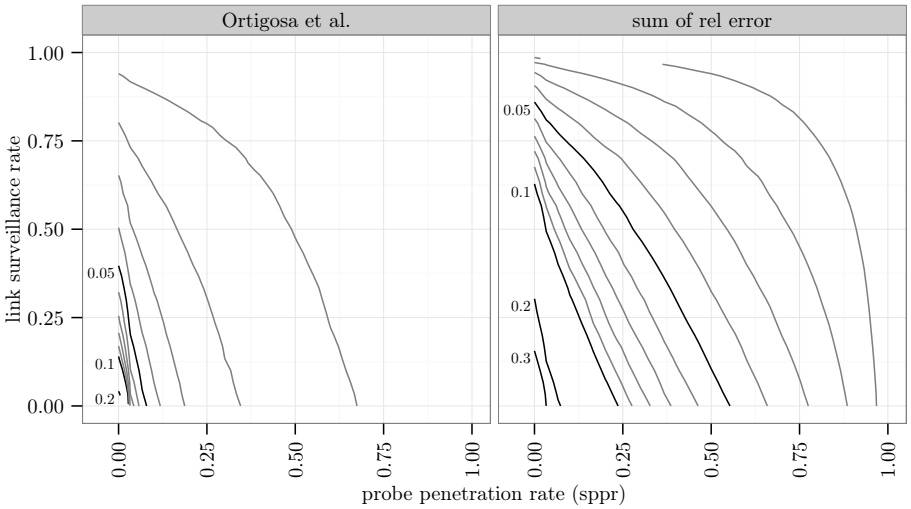

Figure 12: Contour plot of the average 95th quantile error for method 3 (sppr).

rate needs to be estimated, according to section 3.3. Compared to fig. 12, it differs mostly for low levels of link surveillance rates (smaller than 25%), because these cannot ensure an accurate level of probe penetration rate. Again, a fusion is always beneficial.

[12] See footnote 10

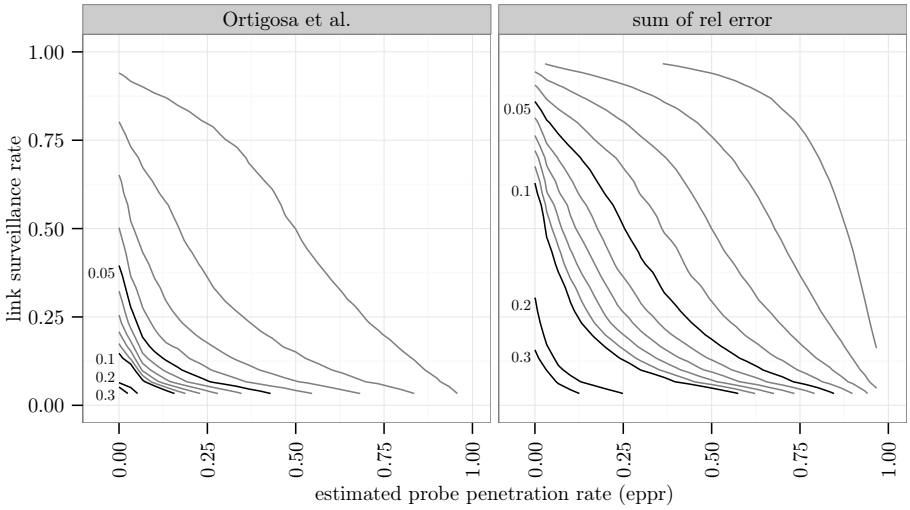

Figure 13: Contour plot of the average 95th quantile error for method 3 (eppr).

4.3.5 Method 4

The results are shown in the same form as for method 1 (for details, cf. 4.3.2). In fig. 14 the contour plots for the fusion method 4 is shown, when probe penetration rates are known a-priori. The errors shown for a probe penetration rate of 0 or a link surveillance rate of 0, represent the errors that would be measured if the data source were on its own. The advantage of this method is that it does not rely on relative numbers, but on absolute observations. The plot shows that fusion method 4 is mostly of advantage for the investigated combinations of network coverages. Both error methods (Ortigosa et al. and sum of the relative errors) differ not only in magnitude. The error after Ortigosa et al. shows similar to method 1 that for the lowest levels of link surveillance, the fusion is not of advantage.

In fig. 15 the contour plot[13] is shown for a network where the probe penetration rate needs to be estimated, according to section 3.3. Compared to fig. 14, it differs mostly for low levels of link surveillance rates (smaller than 25%), because these cannot ensure an accurate level of probe penetration rate. However, it is now always advantageous to fuse the two data sources with method 4.

[13] See footnote 10

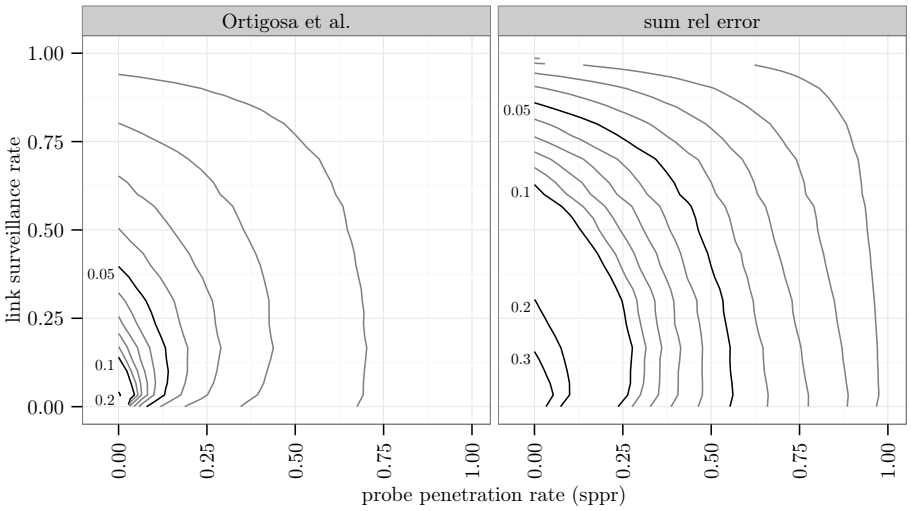

Figure 14: Contour plot of the average 95th quantile error for method 4 (sppr).

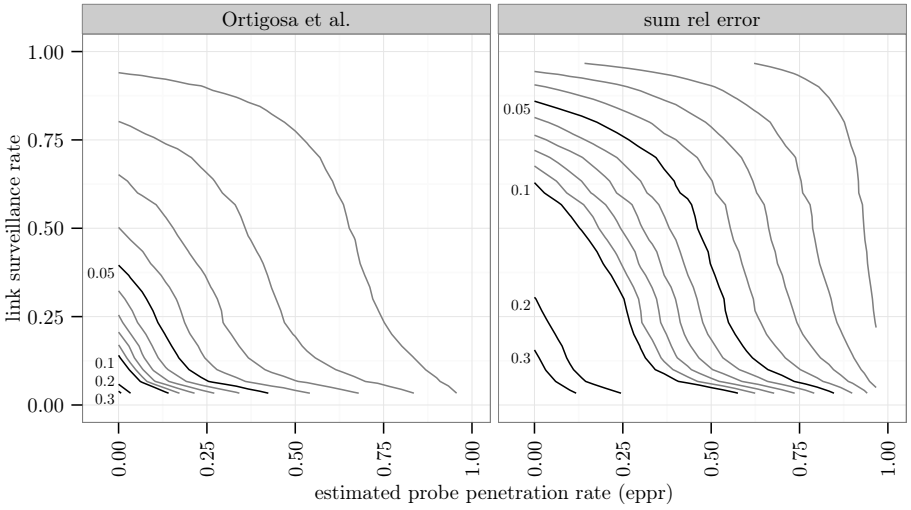

Figure 15: Contour plot of the average 95th quantile error for method 4 (eppr).

4.3.6 Method 5

The results are shown in the same form as for method 1 (for details, cf. 4.3.2). In fig. 16 the contour plots for the fusion method 5 is shown, when probe penetration rates are known a-priori. This somewhat more chaotic plot needs some explanation: As in method 2, some iso error lines are dashed. The probe penetration levels are set at discrete values, the lowest being 1/30. However connecting the errors of a probe penetration rate of 1/30 and of 0 is not completely accurate: It is intuitive from the plot that, for probe penetrations even smaller than 1/30, the error would increase and to indicate this, the connecting iso-error lines are only dashed. This is more obvious for the sum of the relative error method, where the iso-error line with 0.2 shows a sharp downward turn for a probe penetration rate of 1/30. Similar, but less obvious, the same phenomenon can be observed for very low levels of link surveillance rates (for rel. sum error) and for very low levels of probe penetration (for Ortigosa et al.).

When taking a closer look, the errors not only differ in magnitude:
For the error after Ortigosa et al., the fusion method brings no benefits: For a fixed level of probe penetration, an increase in link surveillance has no error decreasing effect. Rather, the error stays at the same level. The explanation is simple: The error after Ortigosa et al. takes only density values into account and the method 5 estimates the network's density only from mobile probes. So, changes in link surveillance do not change the density estimates, thereby not influencing the error after Ortigosa et al.
For a fixed level of link surveillance, an increase in probe penetration rate increases the error at first, to decrease again afterwards (for link surveillance rates > 0.25). This can be seen for a fixed link surveillance rate of 0.75: It starts out with a low error (<0.05), then increases to 0.05 (dark dashed line), and further increases to 0.06 (first solid line in lightgray), and starts decreasing again to 0.05 (dark solid line). This shows that for link surveillance rates higher than 0.25, this method is even counterproductive - it increases the error when fusing. The explanation here, is that for low probe penetrations the fusion relies only on inaccurate density estimates from only little probe vehicles. In the light of the error after Ortigosa et al., fusion method 5 is at best as good as mobile probes on their own, but it can sometimes even worsen the error, than if the sources were to be used not fused.

For the relative sum of the error, similar issues can be observed. For a fixed link surveillance rate of 0.3, it is even clearer than before, with increasing probe penetration rate, the error first increases and decreases afterwards again. However, contrary to the error after Ortigosa et al., this method also takes flow into the error value. For a fixed probe penetration rate, an increasing link surveillance rate, the error increases at first as well. For example for a probe penetration rate of 0.25, the error is 0.1 when the data is not fused. Fusion according to method 5 leads first to higher errors, it crosses the error line of 0.2, and is only at 0.1 again at a link surveillance level of 0.55. So, if the network had 25% probes penetration rate, it would only be able to decrease the error by a fusion with data from at least 55% of the links. In the light of the sum of the relative errors, method 5 is not able to decrease the error compared to the sources on their own for low penetration rate and low link surveillance rates.

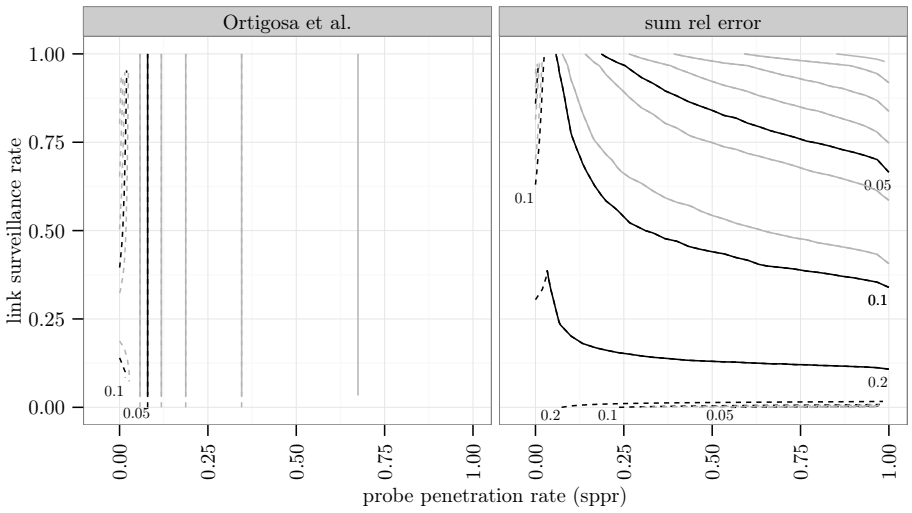

Figure 16: Contour plot of the average 95th quantile error for method 5 (sppr).

In fig. 17 the contour plot[14] is shown for a network where the probe penetration rate needs to be estimated, according to section 3.3. Compared to fig. 16, it differs mostly for the error after Ortigosa et al. where, the lower the link surveillance rate the less accurate is the estimation of the probe penetration rate, and in turn, any estimation from mobile probes. However, as a conservative rule of thumb, it can now be stated that if the estimated probe penetration rate is higher than 10%, a fusion is beneficial, compared to each source on their own.

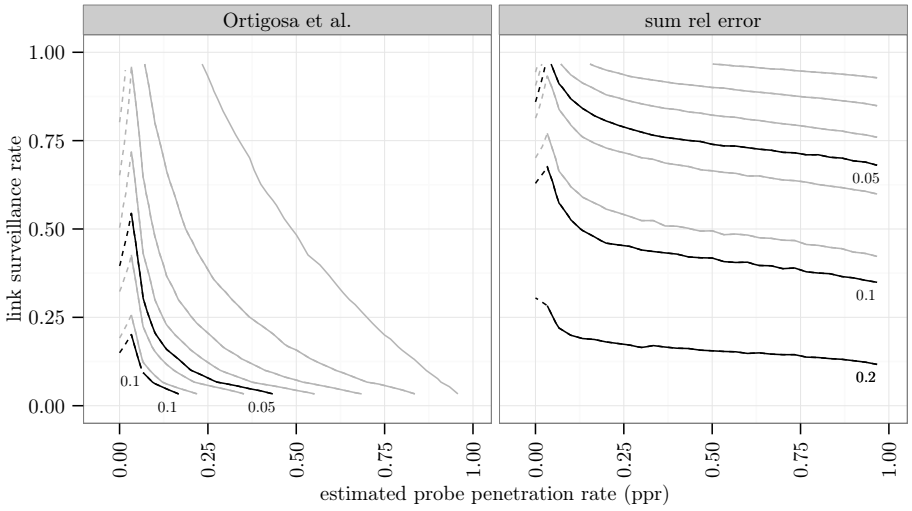

Figure 17: Contour plot of the average 95th quantile error for method 5 (eppr).

[14]See footnote 10

5 Analysis of Results

This section aims at comparing the different fusion method presented in section 3. Firstly, a reference fusion method is introduced, which is based on linear regression and needs perfect information about the MFD. Secondly, a preliminary comparison is made with methods 1-5. And thirdly, based on the aforementioned comparison, a more detailed analysis of the most promising fusion method is given. Furthermore, a comparison in respect to the robustness of specific methods is made.
It has been in explained in sections 2.3 and 3.4 that a for the use of the MFD in a perimeter control system, the errors after Ortigosa et al. are better suited. Therefore, only errors after Ortigosa et al. will be presented in the following. As in section 4.3, the average 95th error of the 5 VISSIM simulations are shown.

Table 2 gives an overview over the results of the fusion methods and the comparison thereof, which are discussed in the following. It is differentiated by the probe penetration rate (ppr) - known and estimated. An efficient method is as a fusion that is *always* better than no fusion. Most of the proposed fusion method are beneficial for some network coverages. However, most fusion methods also have some network coverage combinations for which they increase the investigated errors and are thus not always beneficial (they are inefficient).

Table 2: Analysis of fusion methods in an overview.

Method	**ppr**	**Results**
1	known	Inefficient fusion, especially for low link surveillance rates.
	estimated	Mostly efficient fusion, especially for very low probe penetration rates.
2	known	Inefficient fusion, especially for low probe penetration rates.
	estimated	Same as above.
3	known	Best overall fusion method. Efficient fusion for all investigated network coverages. Robust for measurement errors, not robust for high errors on density values from loop detectors.
	estimated	Same as above.
4	known	Inefficient fusion, especially for low link surveillance rates.
	estimated	Efficient fusion. Performs well for low network coverages.
5	known	Inefficient fusion, especially for low probe penetration rates.
	estimated	Inefficient fusion, except for high errors on density values from loop detectors (very robust).

5.1 Reference Method

In the following, a simple reference method is proposed, which is based on linear regression. As discussed in the methodological part of method 3 in section 3.5.4, it makes sense to split the network in two parts, one with loop detectors and one without. In accordance with section 3.5.4, let $\hat{k}_{l,t}$ denotes the density measured on the sub-network with loop detectors for time slice t, and $\hat{k}_{p-l,t}$ denotes the volume measured by mobile probes on the sub-network without static link surveillance for time slice t. $k_{real,t}$ stands for the real density in the network during time slice t (cf. section 4.2).
For a network perimeter control, the density and the critical density are the decisive variables (cf. sections 2.2 and 3.4). A simple approach is therefore to perform a linear regression with the densities only, by regressing the real density on the density values of loop detectors and probes for each random seed of the VISSIM simulations.
For each combination of link surveillance and probe penetration rate:

$$k_{real,t} = \alpha\hat{k}_{p-l,t} + \beta\hat{k}_{l,t} + \varepsilon \tag{18}$$

This reference method may not be optimal, since depending on what error is used, different regressions need to be applied. For example, for the error after Ortigosa et al., a more complicated quadratic optimization would possibly bring better results. However, the proposed reference method is simple and can be applied with reasonable amount of calculations.

5.2 Comparison of Methods 1-5

5.2.1 Cross-Comparison

In fig. 18 methods 1 - 5 and the reference method are shown in the same plot for probe penetration rates that are known a-priori. For clarity only the iso-error lines for the average 95th quantile with the level of 0.01 (left) and of 0.05 (right; zoom!) were plotted, respectively and the different methods are differentiated with different line types, the reference method is marked in red. When comparing iso-error lines of the same level, a line closer to the origin can be interpreted as a better fusion method: For the same combination of link surveillance rate and probe penetration rate, a lower error can be achieved.
For both iso-error levels it can be observed that methods 1, 4 and 5 do not perform well compared to method 2 and 3. This is not astonishing, since method 1 unnecessarily fuses mobile probe data for links that have already full information based on loop detectors. Method 4 is always outperformed by method 3. And method 5 does not prove to be an efficient fusion method. Method 2 on the other hand shows a good performance for high levels of probe penetration, but for lower ones it gives too much weight to inaccurate values from low probe penetration rates - as already mentioned in section 3.2. For the iso-error line 0.01, method 2 slightly outperforms method 3 for probe penetration levels higher than 0.15. For the iso-error line 0.05, method 3 is clearly outperforming method 2.
Method 3 is for both iso-errors almost as good as the reference method. Thus, for realistically low probe penetration and low link surveillance, method 3 fuses the two sources more efficiently than all other methods investigated.

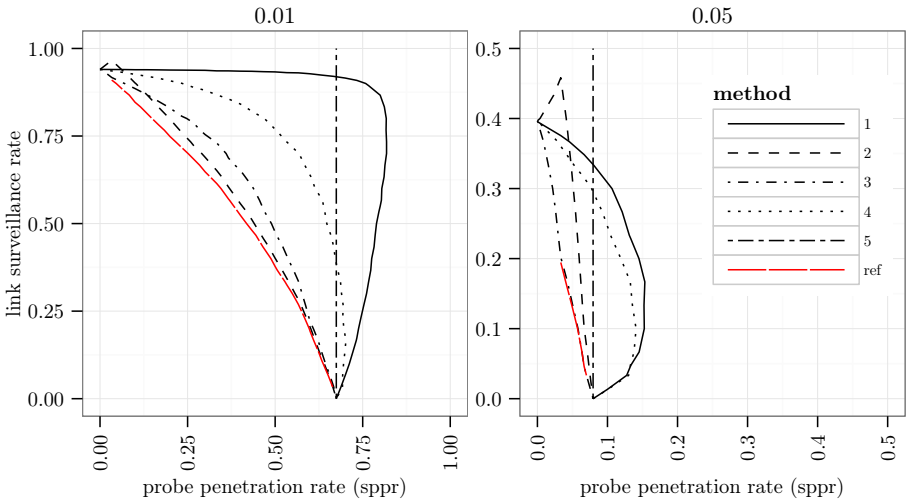

Figure 18: Cross comparison of the average 95th error, iso-error lines 0.01 left, iso-error lines 0.05 right.

In fig. 19 methods 1 - 5 and the reference method (red) are shown in the same plot for probe penetration rates that are not known a-priori. Again, for clarity only the iso-error lines with the level of 0.03 (zoom!) and of 0.1 (zoom!) were plotted, respectively and the different methods are differentiated with different line types.
For the iso-error curve 0.03, method 3 outperforms all others. It follows almost exactly the iso-error line achieved with the reference method. For the iso-curve 0.1, which is interesting for lower levels of network coverage, method 1 and method 4 slightly outperform method 3 and clearly outperform 2 and 1. Compared with the reference method, method 1 and 4 slightly outperform the reference method. This shows that the reference method chosen does indeed not show the optimal fusion, as mentioned in section 5.1.

From the results presented, method 3 is an efficient overall fusion method, as it differs much from the reference method: It is capable of achieving similar fusion results as the reference method. It is only surpassed for unrealistically small probe penetration rates such as 3%. Moreover, method 3 only needs little information (probe penetration and link surveillance rate) compared to the reference method, which needs the real values for the fusion by linear regression. Indeed, a comparison of the weights given to the values of density and flow for the fusion by method 3 and the reference method shows only little difference.

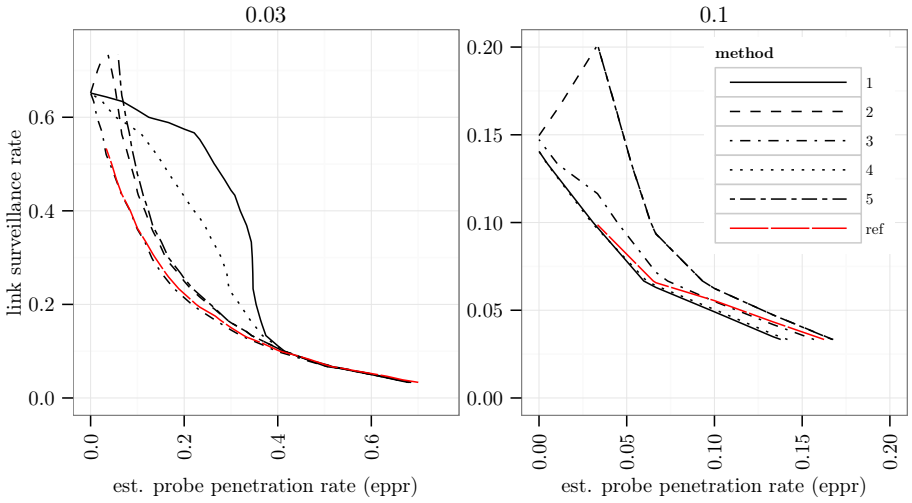

Figure 19: Cross-comparison of the average 95th error, iso-error lines 0.03 left, iso-error lines 0.1 right.

5.2.2 Method 3 and Reference Method

It is possible to further investigate method 3, by splitting the results by the traffic demand. Fig. 20 and 21 show the iso-error plot for a-priori known and estimated probe penetrations, respectively. The iso-error is only labeled for the curves of method 3 and are in intervals of 0.05[15]. The figures show clearly that the demand has two influences. Firstly it shifts the iso-error line (especially for demand 0.3 vs. 0.4-0.6), and secondly, it influences the performance of the fusion.

For fig. 20, method 3 is more or less following the reference method, with demand 0.4 showing the best match of the two. For demand 0.3, the method 3 leads to an inefficient fusion, for the lowest levels of probe penetrations.
For fig. 21, method 3 is again more or less following the the reference method, with the largest inefficiencies for demand 0.3 and 0.6. Both demands in turn show the largest difference between reference method and method 3 for small probe penetration levels with simultaneous small link surveillance. This is expected, since demands 0.3 and 0.6 have lower (average) flows than the other two demands, which leads to a smaller absolute number of probe vehicles in the network making the estimation of the probe penetration rate even more difficult. Low accuracy of the probe penetration rate leads to lower accuracy of the estimated MFD.
In both figures, a clear distinction can be made between the demand 0.3 and the rest of the demands ranging from 0.4 to 0.6. The explanation for this phenomenon lies in the higher congestion heterogeneity that can be assumed with higher demand, making it harder to correctly estimate the MFD, which in turn increases the errors.

[15]For fig. 21: demand 0.3 shows only iso-error lines 0.05 and 0.1 for the reference method.

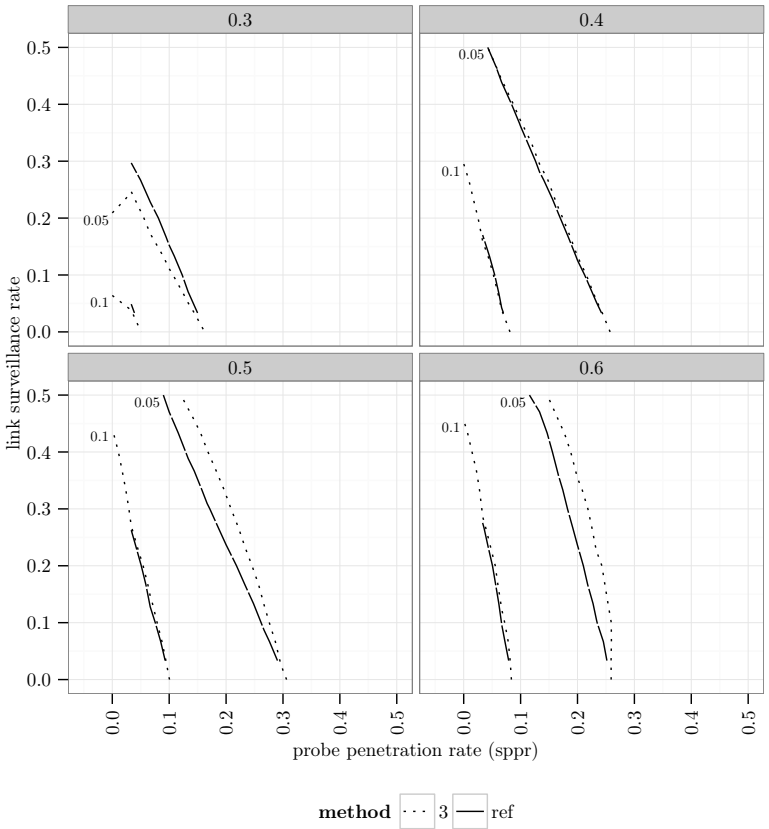

Figure 20: Average 95th error after Ortigosa et al. split up by demand (sppr).

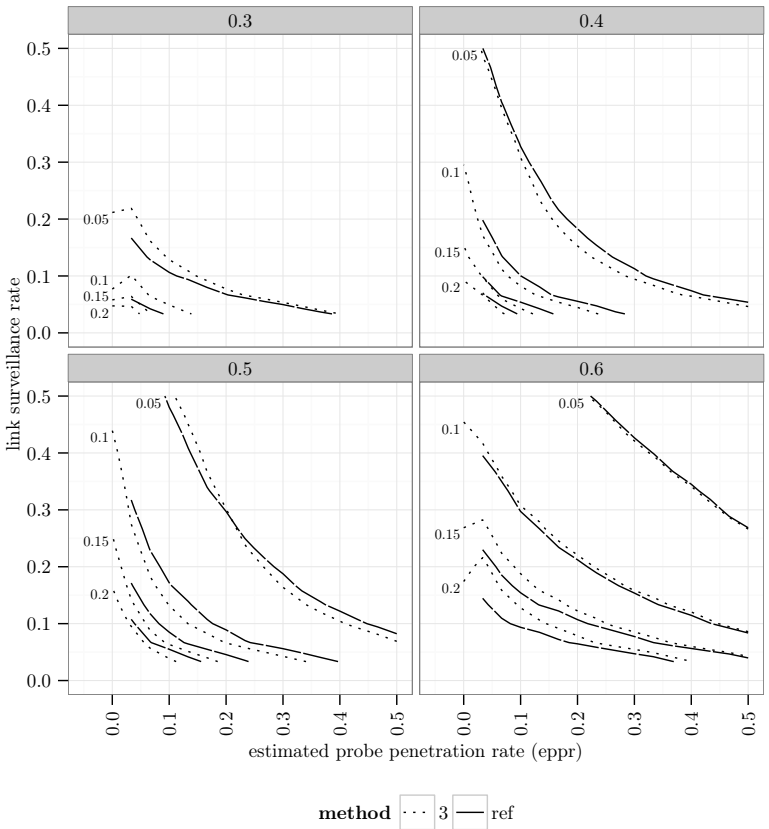

Figure 21: Average 95th error after Ortigosa et al. split up by demand (eppr).

5.3 Robustness of Methods 3 and 5

In reality mobile probe data and loop detectors can be seriously flawed - due to either measurement errors and due to the position of the detector within the link. This section aims at comparing the robustness of method 3 and method 5. Method 3 was chosen, since it has a good overall performance. And, method 5 was chosen because it does incorporate an approach possibly more related to practice, taking the flow from loop detectors and taking the density from the mobile probes. Loop detectors are only capable of measuring density accurately under certain conditions explained in section 2.3 and 3.5.

5.3.1 Measurement Errors

In the following, synthetic measurement errors assumed to be normally distributed are introduced. For every probe vehicle an error following $\alpha \cdot value$ is introduced on its distance and time spent in the network, where α follows $\mathcal{N}(1, 0.1)$. And, also for each density and flow value measured by a loop detector, an error is multiplied, $\beta \cdot value$, where β follows a normal distribution $\mathcal{N}(1, 0.1)$. Since the MFD aggregates the density and the flow on the network, by taking the average time and distance spent of probes or by averaging the density and flow values measured by loop detectors, a closer look at the error propagation needs to be taken.
Given a sample of n independent random variables $X_1, X_2, \ldots, X_n$. Each variable is a randomly drawn observation with the distribution of the population, with mean μ and standard deviation σ. Then the sample mean is $\bar{x} = n^{-1} \sum_{i=1}^{n} X_i$ and the sample standard deviation is $\sigma_{sample} = n^{-1/2}\sigma$ (compare for example (Barlow, 2013)).
Under the assumption that the loop detector errors are independent, it is possible to state the following equations for network averages:

$$\textit{for probes: } q_{err,p} = \alpha \hat{q}_p \qquad \textit{with } \alpha \textit{ following } \mathcal{N}\left(1, \frac{0.1}{\sqrt{N_p}}\right) \tag{19}$$

$$\textit{for loops: } q_{err,l} = \beta \hat{q}_l \qquad \textit{with } \beta \textit{ following } \mathcal{N}\left(1, \frac{0.1}{\sqrt{180\phi}}\right) \tag{20}$$

where $\hat{q}_l$ and $q_{err,l}$ are the average estimated network flow measured by loop detectors with and without including a synthetic measurement error, respectively. ϕ is the link surveillance rate and 180 is the total number of links in the network. The standard deviation of the average flow is inversely proportional to the square root of the number of links used to estimate the average flow. This is analogue for mobile probes, where the standard deviation is inversely proportional to the square root of the number of mobile probes, N_p. Identical considerations are made for the density measures.

Fig. 22 shows method 3 and method 5[16] in cross-comparison, when the probe penetration rate is known (left), and when the probe penetration rate needs to be estimated (right). It can be observed that both fusion methods exhibit almost

[16] For clarity, method 5 is shown without the iso-error curves for a probe penetration rate at 0. If necessary, they can be seen in section 4.3.

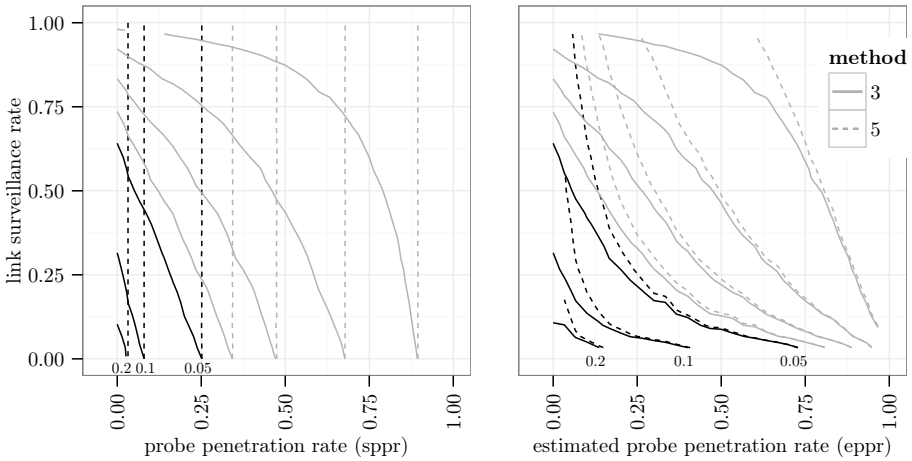

Figure 22: Average 95th error of methods 3 and 5 when inducing a measurement error.

no change in their average 95th quantile errors compared to without synthetic errors. With the synthetic error, method 3 is still performing much better than method 5. Method 3 is robust against the assumed measurement errors. The reason is that the standard deviation is inversely proportional to the number of observations making up the average. For example, for a probe penetration of 0.1, there are around 500 probe vehicles in the network (for one time slice), and the standard deviation is around 0.004 for the distribution introduced above.

5.3.2 Loop Density Errors

In the following, a synthetic error is induced only to the density values of the loop detectors, simulating thereby the variation in density due to the position of the detector within the link. *For this experiment, the assumptions from section 3.1 stating that loop detectors are well distributed within the links is relaxed.* For example, if most loop detectors are positioned close to an intersection, the accuracy of the density measurement is overestimated. Courbon and Leclercq (2011) showed that, averages from loop detectors may overestimate up to 100% of the real value, depending on flow.
For further analysis a benchmark of 50% overestimation is defined. For each density, measured by a loop detector, an error is multiplied, $\gamma \cdot \hat{k}_l$, where γ follows a normal distribution $\mathcal{N}(1.5, 0.1)$. This alters eq. 20 to:

$$\textit{for loops: } k_{err,l} = \gamma \hat{k}_l \qquad \textit{with } \gamma \textit{ following } \mathcal{N}\left(1.5, \frac{0.5}{\sqrt{180\phi}}\right) \tag{21}$$

$$\tag{22}$$

Fig. 23 shows method 3 and method 5 in cross-comparison, when the probe penetration rate is known (left), and when the probe penetration rate needs to be estimated (right). In any case method 5 is better than method 3. As

mentioned earlier, the closer to the origin, the better the fusion. Method 3 is always further away from the origin, thus, it is less efficient than method 5. As assumed in section 3.5, method 5 is robust against distortions of the density measurement due to the placement of the loop detectors within the links, since densities are estimated by mobile probes only. One interesting observation is that compared to section 3.5, it is not a disadvantage anymore to fuse data with method 5. This is due to the high error on loop detectors.
Method 3 should not be used for fusion. Except for low link surveillance rates and *estimated* probe penetration rates lower than 50% if the probe penetration rate is estimated: The fact that the probe penetration rate needs to be estimated makes the iso-error curve turn, making it possible for method 5 to be beneficial for this small portion of the network coverage. However as a concluding remark, method 3 is not robust for large density errors induced by the position of the loop detector. Method 5 proves to be a very robust method.

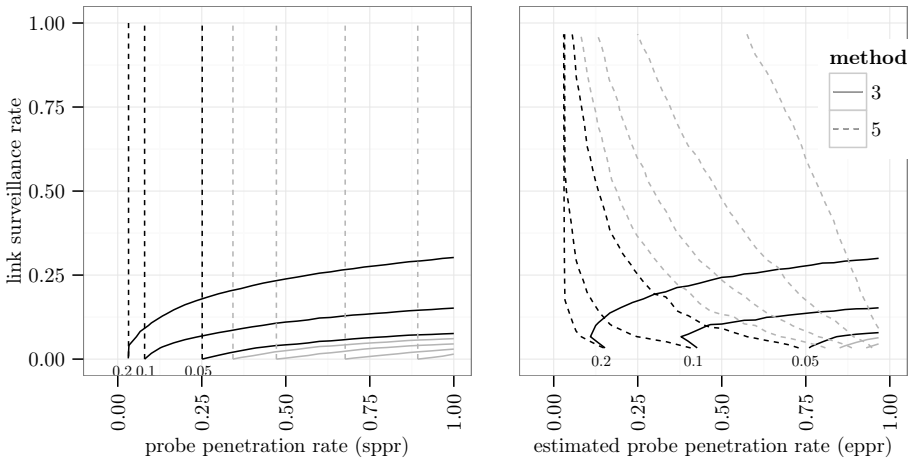

Figure 23: Average 95th error of methods 3 and 5 when inducing an error on density values from loop detectors.

6 Conclusions

Congestion in the Canton of Zurich alone produces costs to each inhabitant of around CHF 100 a year. With recent research developments such as the macroscopic fundamental diagram (MFD), cities have a simple and easy-to-use tool to not only monitor but also manage traffic. The MFD is compact and gives an aggregated view of traffic conditions within a city which can feed well known traffic management systems, such as a perimeter control. However, the MFD is dependent on accurate data.
In recent literature, the estimation of the MFD with only limited network coverage has gained interest. Different sources of data were examined separately, with loop detectors and floating car data being the two most prominent ones. Each of them was analyzed in respect to the network coverage and possible methods of estimating the MFD accurately. However, in reality the aforementioned data sources are available simultaneously: Some links have loop detectors and some vehicles or drivers have devices that make it possible to track them.
The novelty of this master's thesis lies in the proposed fusion methods, where both loop detectors and floating car data are used simultaneously to estimate the MFD. The comparison of the fused data with stand-alone data (i.e. loop detectors or floating car data on their own) shows that data fusion indeed leads to an estimated MFD containing lower errors than if it were estimated solely based on loop detectors *or* floating car data. With the results presented in this master's thesis cities will now be capable of much better leveraging the different information generated by loop detectors and floating car data. With the presented fusion methods, cities can not only estimate the MFD more accurately, but also cost efficiently, by knowing exactly how many loop detectors and how much floating car data are needed for which accuracy level.

6.1 Main Findings

The following gives a more detailed overview of the main findings:

i When estimating the probe penetration rate:

- How well the probe penetration rate (what fraction of vehicles can be tracked) can be estimated depends on the link surveillance rate (what fraction of links have a loop detector installed) and also on the probe penetration itself.
- The higher the link surveillance rate and the higher the probe penetration rate, the lower the error of the estimation will be.

ii When estimating the MFD based on one source only:

- For the same level of network coverage, the MFD based solely on mobile probes shows lower errors than the MFD based solely on loop detectors.
- It is found the higher the demand in the network is, the even more superior the estimation based on mobile probes is, compared to a loop detector based estimation. For the same network coverage, mobile probes are consistently superior registering the heterogeneity in

congestion. This can be attributed to the better spatial distribution of mobile probes.

iii When estimating the MFD based on loop detectors and mobile probes simultaneously:

- In general, the MFD estimation based on the fusion of the two data sources is often better than the estimation based solely on one data source. This applies in particular if probe penetration rates need to be estimated.
- Fusion method 3 always leads to a better estimation of the MFD, compared with an estimation based solely on one data source (for the investigated network coverage). It fuses according to the network coverage of the loop detectors and the square root of the probe penetration rate. It is also almost as good as a simple reference method based on linear regression, which would require knowledge of the real MFD.
- Fusion method 1, 2, 4 and 5 sometimes lead to an MFD estimation which is better, identical or worse than an estimation based on only one data source, depending on the chosen error, on the a-priori knowledge of the probe penetration rate and on the network coverage.

iv When inducing synthetic errors:

- Method 3 is robust against small synthetic measurement errors.
- When inducing large synthetic errors to the density estimated by loop detectors, fusion method 3 cannot be considered robust. Rather, it is fusion method 5 that leads to consistent and robust results.

Summa summarum:

If loop detectors are well distributed within the links, already a simple fusion following the schemes of method 3, improves the estimated MFD significantly.

6.2 Future Research

The presented methods and results can be seen as a first approach to use both, loop detectors and floating car data simultaneously to estimate the MFD. Further developments are necessary, which can be categorized in two fields: Experimental setup and fusion method.

Although, the proposed experimental setup is based on a realistic grid network, it has to be shown that the results presented are completely transferable to a real one. As stated multiple times, the loop detectors in this setup are assumed to be well distributed within the links. It should be envisaged to distribute loop detectors in specific manners (all loop detectors close to the intersection, etc.). The mobile probe vehicles were homogeneously distributed. Further analysis about the impact of such an assumption are needed.

This research can be seen as a preliminary approach fusing data to obtain a more accurate MFD. It remains to be shown that estimating the MFD with density and flow, based on mobile probes of unknown penetration rate, is more efficient than using the information of mobile probes for the estimation of average speed in the network and the loop detectors for the estimation of average flow. The very low accuracy of the latter method has been discussed in section 2.3, but it was not compared to the method implemented in this master's thesis. Also, a better understanding of the relation between the accuracy of the estimation of probe penetration rates and the accuracy of the MFD could possibly reveal a superior fusion method.
More efficient fusion methods might be found, when more parameters are taken into account. Most promising examples are time dependent (extended) Kalman filters or different fusing methods for different traffic states. However, the drawbacks of such, much more complex methods, are usually that more input variables are needed, which sometimes in reality do not exist. Another option would be to apply two different fusion methods, one for the congested branch and one for the uncongested branch of the MFD. Furthermore, an approach could be taken that optimizes the perimeter control scheme. Thereby, other accuracy indicators could be used, such as the network delay (cf. section 2.3). In any case, it is important to understand that the quality of the fusion method depends significantly on the goal of it.

Bibliography

ASTRA (2014). Verkehrsentwicklung und Verfuegbarkeit der Nationalstrassen. Technical report, Swiss Federal Road Office, ASTRA.

Barlow, R. J. (2013). *Statistics - A Guide to the Use of Statistical Methods in the Physical Sciences*. John Wiley, Sons, New York.

Buisson, C. and Ladier, C. (2009). Exploring the impact of homogeneity of traffic measurements on the existence of macroscopic fundamental diagrams. *Transportation Research Record: Journal of the Transportation Research Board*, 2124(1):127–136.

Courbon, T. and Leclercq, L. (2011). Cross-comparison of macroscopic fundamental diagram estimation methods. *Procedia-Social and Behavioral Sciences*, 20:417–426.

Daganzo, C. F. (2007). Urban gridlock: macroscopic modeling and mitigation approaches. *Transportation Research Part B: Methodological*, 41(1):49–62.

Daganzo, C. F. and Geroliminis, N. (2008). An analytical approximation for the macroscopic fundamental diagram of urban traffic. *Transportation Research Part B: Methodological*, 42(9):771–781.

Ernst Basler+Partner (2008). Wie weiter mit dem Verkehr? Technical report, Zurich Cantonal Bank.

Gayah, V. V. and Dixit, V. V. (2013). Using mobile probe data and the macroscopic fundamental diagram to estimate network densities. *Transportation Research Record: Journal of the Transportation Research Board*, 2390(1):76–86.

Geroliminis, N. and Daganzo, C. F. (2007). Macroscopic modeling of traffic in cities. In *TRB 86th annual meeting*, number 07-0413.

Geroliminis, N. and Daganzo, C. F. (2008). Existence of urban-scale macroscopic fundamental diagrams: Some experimental findings. *Transportation Research Part B: Methodological*, 42(9):759–770.

Geroliminis, N. and Sun, J. (2011). Properties of a well-defined macroscopic fundamental diagram for urban traffic. *Transportation Research Part B: Methodological*, 45(3):605–617.

Godfrey, J. (1969). The mechanism of a road network. *Traffic Engineering & Control*, 8(8).

Greenshields, B., Channing, W., Miller, H., et al. (1935). A study of traffic capacity. In *Highway research board proceedings*, volume 1935. National Research Council (USA), Highway Research Board.

Hall, R. (2012). *Handbook of transportation science*, volume 23. Springer Science & Business Media.

Herman, R. and Prigogine, I. (1979). A two-fluid approach to town traffic. *Science*, 204(4389):148–151.

Keller, M. and Wuethrich, P. (2012). Neuberechnung der Stauzeitkosten. Technical report, infras, ARE.

Leclercq, L., Chiabaut, N., and Trinquier, B. (2014). Macroscopic fundamental diagrams: A cross-comparison of estimation methods. *Transportation Research Part B: Methodological*, 62:1–12.

Mazloumian, A., Geroliminis, N., and Helbing, D. (2010). The spatial variability of vehicle densities as determinant of urban network capacity. *Philosophical Transactions of the Royal Society of London A: Mathematical, Physical and Engineering Sciences*, 368(1928):4627–4647.

Mitchell, H. B. (2007). *Multi-sensor data fusion: an introduction*. Springer Science & Business Media.

Nagle, A. S. and Gayah, V. V. (2014). Accuracy of Networkwide Traffic States Estimated from Mobile Probe Data. *Transportation Research Record: Journal of the Transportation Research Board*, 2421(1):1–11.

Nagle, A. S. and Gayah, V. V. (2015). Comparing the use of link and probe data to inform perimeter metering control. In *Transportation Research Board 94th Annual Meeting*, number 15-0621.

Ortigosa, J., Menendez, M., and Gayah, V. V. (2015). Analysis of Network Exit Functions for Different Urban Grid Network Configurations. In *Transportation Research Board 94th Annual Meeting*, number 15-2886.

Ortigosa, J., Menendez, M., and Tapia, H. (2014). Study on the number and location of measurement points for an MFD perimeter control scheme: a case study of Zurich. *EURO Journal on Transportation and Logistics*, 3(3-4):245–266.

PTV (2014). *Vissim 7 User Manual*. PTV AG, Karlsruhe, Germany.

Smeed, R. J. (1968). Traffic studies and urban congestion. *Journal of Transport Economics and Policy*, pages 33–70.

Thomson, J. M. (1967). *Speeds and Flows of Traffic in Central London...* Printerhall.

A Annex

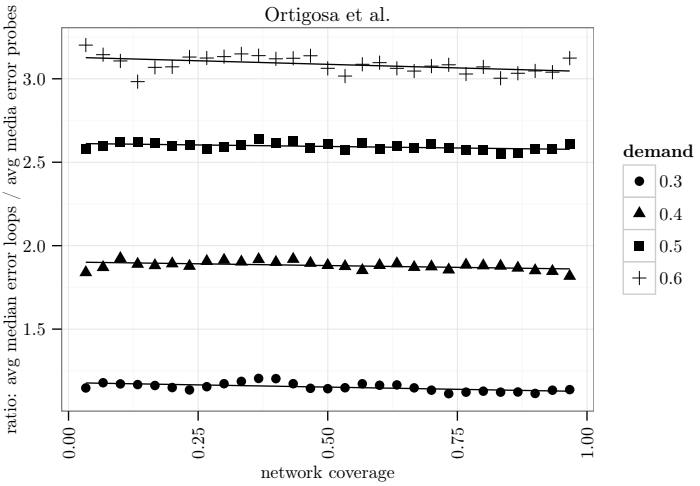

Figure 24: Average median error ratio, Ortigosa et al.

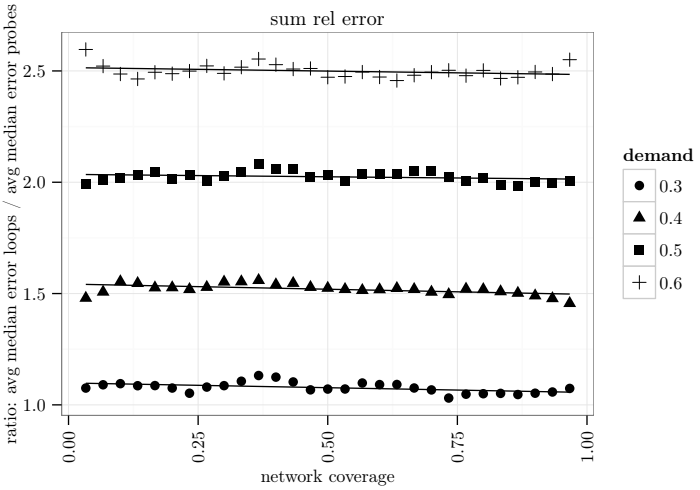

Figure 25: Average median error ratio (not per surveyed vehicle!).

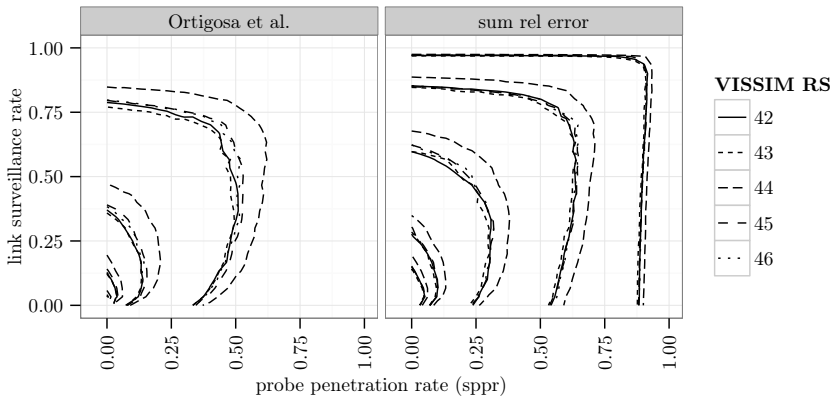

Figure 26: 95th error different VISSIM random seeds for fusion method 1 (sppr).

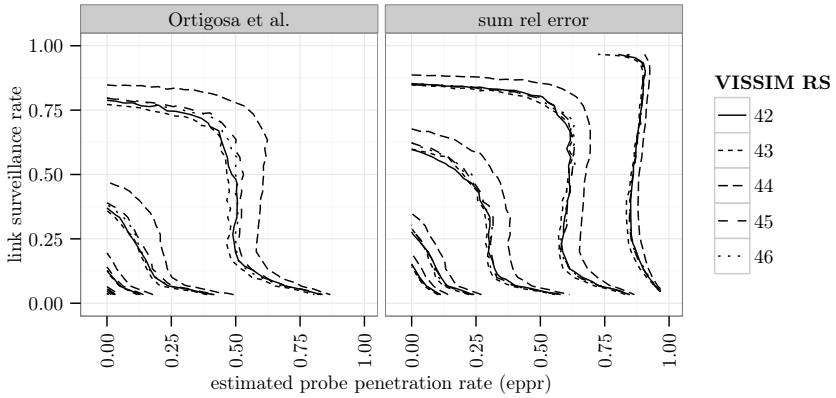

Figure 27: 95th error different VISSIM random seeds for fusion method 1 (eppr).

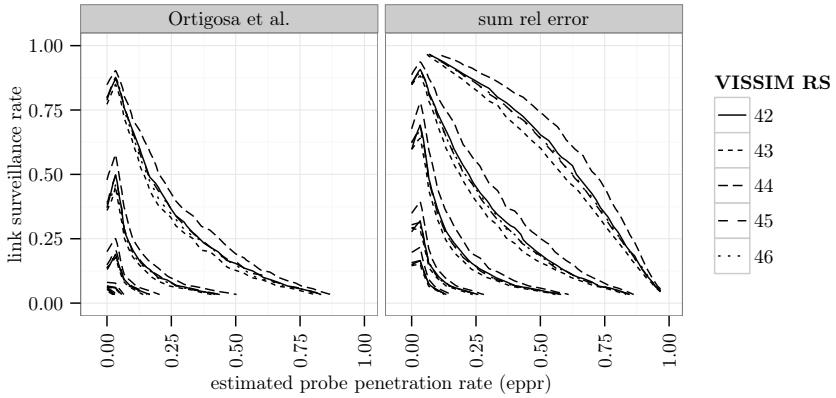

Figure 28: 95th error different VISSIM random seeds for fusion method 2 (sppr).

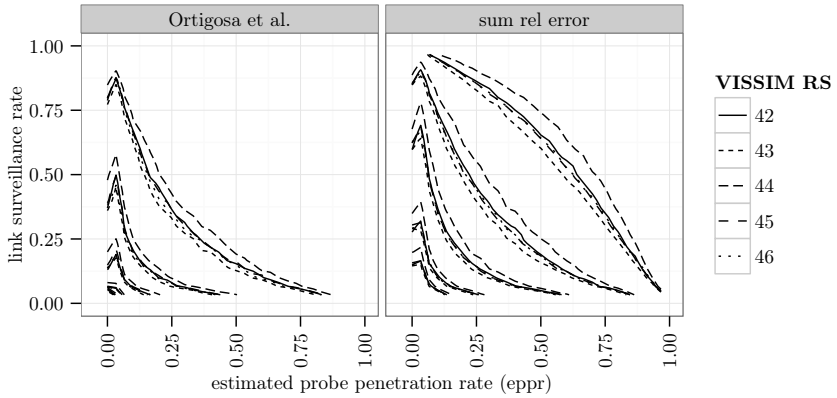

Figure 29: 95th error different VISSIM random seeds for fusion method 2 (eppr).

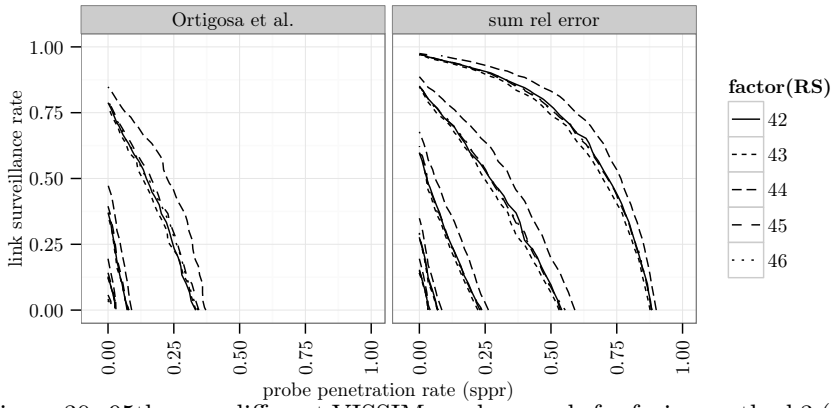

Figure 30: 95th error different VISSIM random seeds for fusion method 3 (sppr).

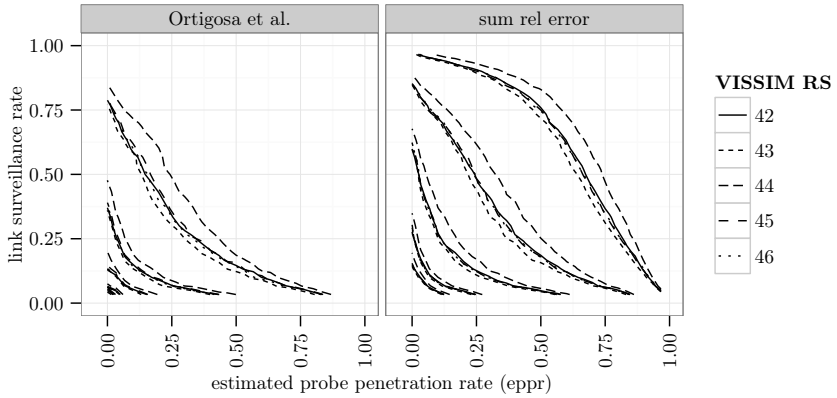

Figure 31: 95th error different VISSIM random seeds for fusion method 3 (eppr).

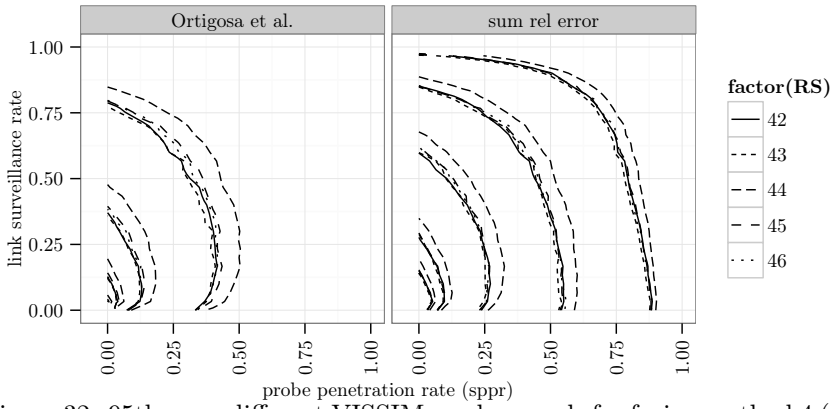

Figure 32: 95th error different VISSIM random seeds for fusion method 4 (sppr).

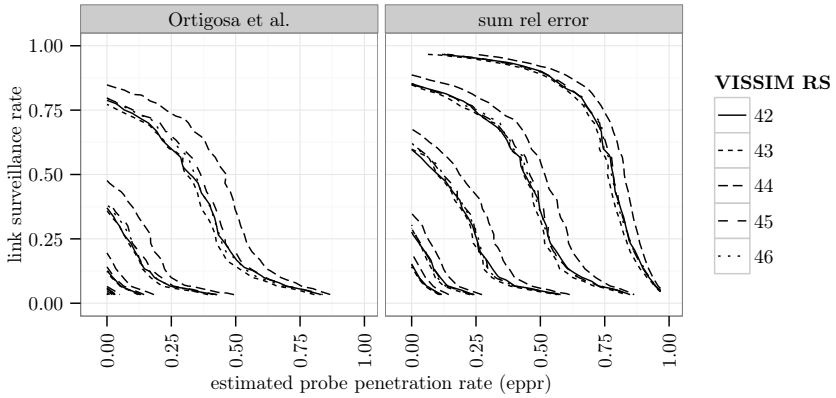

Figure 33: 95th error different VISSIM random seeds for fusion method 4 (eppr).

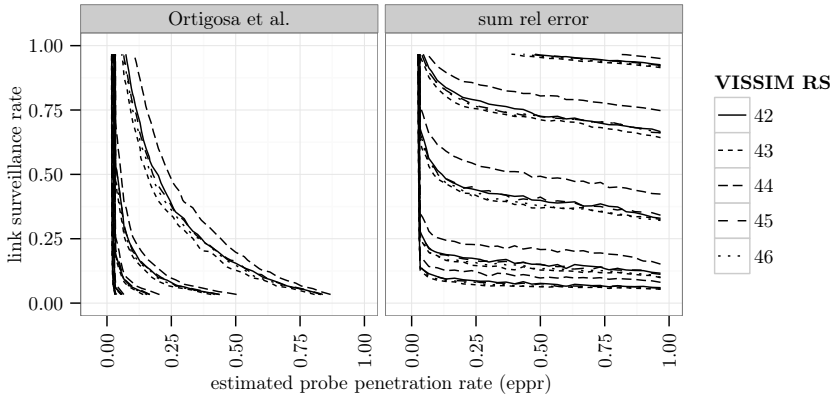

Figure 34: 95th error different VISSIM random seeds for fusion method 5 (sppr).

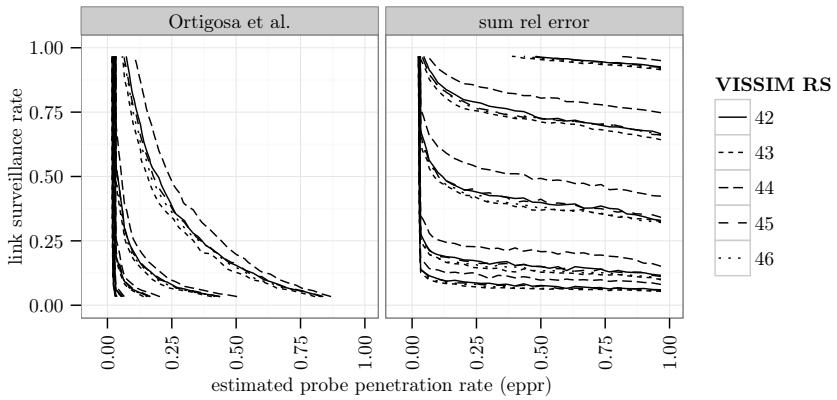

Figure 35: 95th error different VISSIM random seeds for fusion method 5 (eppr).

Eidgenössische Technische Hochschule Zürich
Swiss Federal Institute of Technology Zurich

Declaration of originality

The signed declaration of originality is a component of every semester paper, Bachelor's thesis, Master's thesis and any other degree paper undertaken during the course of studies, including the respective electronic versions.

Lecturers may also require a declaration of originality for other written papers compiled for their courses.

I hereby confirm that I am the sole author of the written work here enclosed and that I have compiled it in my own words. Parts excepted are corrections of form and content by the supervisor.

Title of work (in block letters):

Authored by (in block letters):
For papers written by groups the names of all authors are required.

Name(s):	**First name(s):**

With my signature I confirm that

- I have committed none of the forms of plagiarism described in the 'Citation etiquette' information sheet.
- I have documented all methods, data and processes truthfully.
- I have not manipulated any data.
- I have mentioned all persons who were significant facilitators of the work.

I am aware that the work may be screened electronically for plagiarism.

Place, date	**Signature(s)**

For papers written by groups the names of all authors are required. Their signatures collectively guarantee the entire content of the written paper.